UNIVERSITY OF BIRMINGHAM

Functional Consequences of Threonine-60 Phosphorylation of Pituitary-Tumor Transforming Gene

and

The Role of Vascular Endothelial Growth Factor in Decidualisation

Jessica Foster

Submitted for Master's of Research (MRes) Degree

College of Medical and Dental Sciences

University of Birmingham

May 2013

UNIVERSITY OF BIRMINGHAM

PROJECT ONE:

Functional Consequences of Threonine-60 Phosphorylation of Pituitary-Tumor Transforming Gene

This project is submitted in partial fulfilment of the requirements for the award of MRes Biomedical Research

This project was carried out under the supervision of:

Professor Chris McCabe

Abstract

Pituitary-tumour transforming gene (PTTG), or human Securin, is an integral part of the spindle assembly checkpoint machinery in mitosis. It is often over-expressed in cancer, and is a prognostic marker for many cancer types. PTTG mutational status, however, has not been explored until very recently. A Threonine-60 mutation in PTTG has recently been highlighted as inducing chromosomal instability, and increased invasiveness (Mora-Santos et al., 2013). This study hypothesises that phosphorylation at the Threonine-60 residue modulates PTTG degradation in mitosis, particularly in respect to its interaction with the anaphase promoting complex/cyclosome (APC/C). We aimed to investigate this hypothesis using both WT PTTG and PTTG forms mutated at the T60 residue through a variety of protein biochemistry techniques, predominantly investigating the interaction between the APC/C co activator Cdc20 and the ubiquitination potential of these proteins. Results indicate that mutation of the T60 site does not abrogate ubiquitination by the APC/C and increases binding to Cdc20 compared to that of WT PTTG.

Acknowledgements

I would like to thank Professor Chris McCabe for all his guidance and support throughout my time in his lab. Thank you to Dr Andy Turnell for his help and advice., and thanks also to all of the McCabe lab, particularly Vikki Poole, Bhavika Modasia and Gavin Ryan, for their encouragement and patience.

Table of Contents

1.0 INTRODUCTION 8

1.1 THE CELL CYCLE 8

1.2 MITOSIS 11

1.3 SPINDLE ASSEMBLY CHECKPOINT 11

1.3.1 The Anaphase Promoting Complex/Cyclosome 13

1.3.2 Separase and Securin 16

1.3.3 The Mitotic Checkpoint Complex and Cdc20 17

1.4 HUMAN SECURIN - THE PITUITARY TUMOR-TRANSFORMING GENE 18

1.5 PTTG MUTATIONS 20

1.7 AIMS AND OBJECTIVES 22

2.0 MATERIALS AND METHODS 23

2.1 CELL LINES AND TISSUE CULTURE CONDITIONS 23

2.1.1 Cell Lines 23

2.1.2 Tissue Culture 23

2.2 PLASMIDS AND TRANSIENT TRANSFECTIONS 24

2.2.1 Plasmids 24

2.2.2 Transient Transfections 24

2.2.3 Protein Harvesting 26

2.3 TRANSFECTION AND ANTIBODY VALIDATION 26

2.3.1 Sample Preparation 26

2.3.2 SDS-PAGE 27

2.3.3Western Blotting 28

2.4 CO-IMMUNOPRECIPITATION 30

2.4.1 Cell Synchronisation *30*

2.4.2 Protein Harvesting and Co-Immunoprecipitation *30*

2.4.3 SDS-PAGE and Western Blotting *31*

2.5 *IN VITRO* STUDIES 33

2.5.1 L-α-[^{35}S]-Methionine Radiolabelled in vitro Protein Synthesis *33*

2.5.2 Ubiquitination Assay *33*

2.5.3 GST-Pulldown Assay *35*

3.0 RESULTS 36

3.1 EXPRESSION OF PTTG MUTANTS IN TPC1 CELLS 36

3.2 INVESTIGATING THE INTERACTION BETWEEN PTTG MUTANTS AND CDC20 36

3.3 PTTG MUTANTS ARE SUBSTRATES FOR APC/C-DIRECTED UBIQUITIN LIGASE ACTIVITY 40

3.4 INVESTIGATING THE INTERACTION OF THE PTTG MUTANTS AND APC/C SUBUNITS *IN VITRO* 43

3.5 ANTIBODY VALIDATION 45

4.0 DISCUSSION 49

5.0 REFERENCES 53

List of Figures and Tables

Figure 1: The Cell Cycle 9

Figure 2: The Stages of Mitosis 10

Figure 3: The Spindle Assembly Checkpoint 12

Figure 4: The E1, E2 and E3 Ubiquitination Pathway 14

Figure 5: PTTG Domain Map 21

Table 1: List of Plasmids 25

Table 2: List of Antibodies 29

Figure 6: Transfection of WT and Mutant PTTG in TPC1 Cells 37

Figure 7: Preliminary myc-Cdc20-PTTG Co-IP in Asynchronous HeLa Cell 38

Figure 8: Replicate myc-Cdc20-PTTG Co-IP in Synchronised HeLa Cells 39

Figure 9: Ubiquitination of APC/C Substrates Cyclin A and Cyclin B 41

Figure 10: Ubiquitination of WT PTTG and mutant PTTG 42

Figure 11: GST-Pulldown Assay of GST-APC3 and GST-Cdc20 with PTTG 44

Figure 12: Validation of Day 53 Polyclonal T60 Phospho-Specific Antibody Bleed 46

Figure 13: Validation of Day 88 Polyclonal T60 Phospho-Specific Antibody Bleed 47

1.0 Introduction

1.1 The Cell Cycle

The cell cycle is a highly regulated, dynamic process. Normally, cells enter the cell cycle in response to cellular or environmental signals, and only undergo successful cell division if specific requirements and checkpoints are satisfied. Four main stages make up the cell cycle; G1 phase, where organelles and other cell components are duplicated; S phase, where DNA replication occurs; G2 phase, where the DNA is proof read and metabolic changes take place; and M phase, or mitosis, where the cell divides (Figure 1).

The importance of strict control of the cell cycle has been understood to a certain extent for many years, with the first recorded observation of abnormal cell division in cancer made in 1914 by Theodor Boveri. Since then pioneering discoveries such as the Cdc (cell cycle division) proteins, cyclins and Cdks (cyclin dependant kinases), along with the presence of cell cycle checkpoints have helped understanding in this field grow exponentially (Nurse P., 1975; Evans et Al., 1983; Hartwell & Weinhart, 1989).

The cell cycle has many regulatory points including, the G1 to S transition, the G2 to M phase transition and the Metaphase to Anaphase transition in mitosis. These regulatory processes are critical in the prevention of the abnormal cell division that can lead to the uncontrollable proliferation seen in cancer cells, and are particularly crucial to ensure cells undergo ‘normal’ mitosis.

Figure 1: The Cell Cycle

Figure 1: The cell cycle. The different stages involved, in the cell cycle and the changes that occur during these stages (Source: University of Leicester (2013))

Figure 2: The Stages of Mitosis

Figure 2: The stages of mitosis. Individual stages of mitosis, and the alterations that occur (Source: University of Leicester (2013))

1.2 Mitosis

Mitosis, or M phase, is comprised of five main stages – prophase, prometaphase, metaphase, anaphase and telophase (Figure 2). As cells enter prophase from G2 phase the nuclear envelope breaks down, chromosomes condense and spindle fibres begin to form. These spindle fibres begin to attach to kinetochores at the centromeres of the condensed chromosomes in prometaphase, and align upon the metaphase plate during metaphase (Ault & Nicklas, 1998) (Figure 2 and 3). At this point the spindle assembly checkpoint (SAC) must be satisfied for the cells to enter anaphase. For this to occur all chromosomes must be aligned upon the metaphase plate in a bi-orientated manner, and all chromosome kinetochores attached to spindle fibres (Reider et al., 1994; Reider et al., 1995). Once these requirements have been met the cells progress into anaphase where the Cohesion complex between sister chromatids is cleaved and sister chromatids move to opposing ends of the cell (Clute & Pines, 1999; Bagting et al., 2002) (Figure 2 and 3). The nuclear envelopes reform in telophase, and ready the cell for cytoplasm division by cytokinesis (Figure 2).

1.3 Spindle Assembly Checkpoint

The spindle assembly checkpoint (SAC) is the main cell cycle checkpoint in mitosis. Simplistically it monitors the attachment of kinetochores to the spindle fibres, and is sensitive enough to even detect a single unattached spindle (Reider et al., 1994; Reider et al., 1995). The tension exhibited upon the kinetochores and spindle fibres is an important signal indicative of spindle attachment, and until signals are received that

Figure 3: The Spindle Assembly Checkpoint

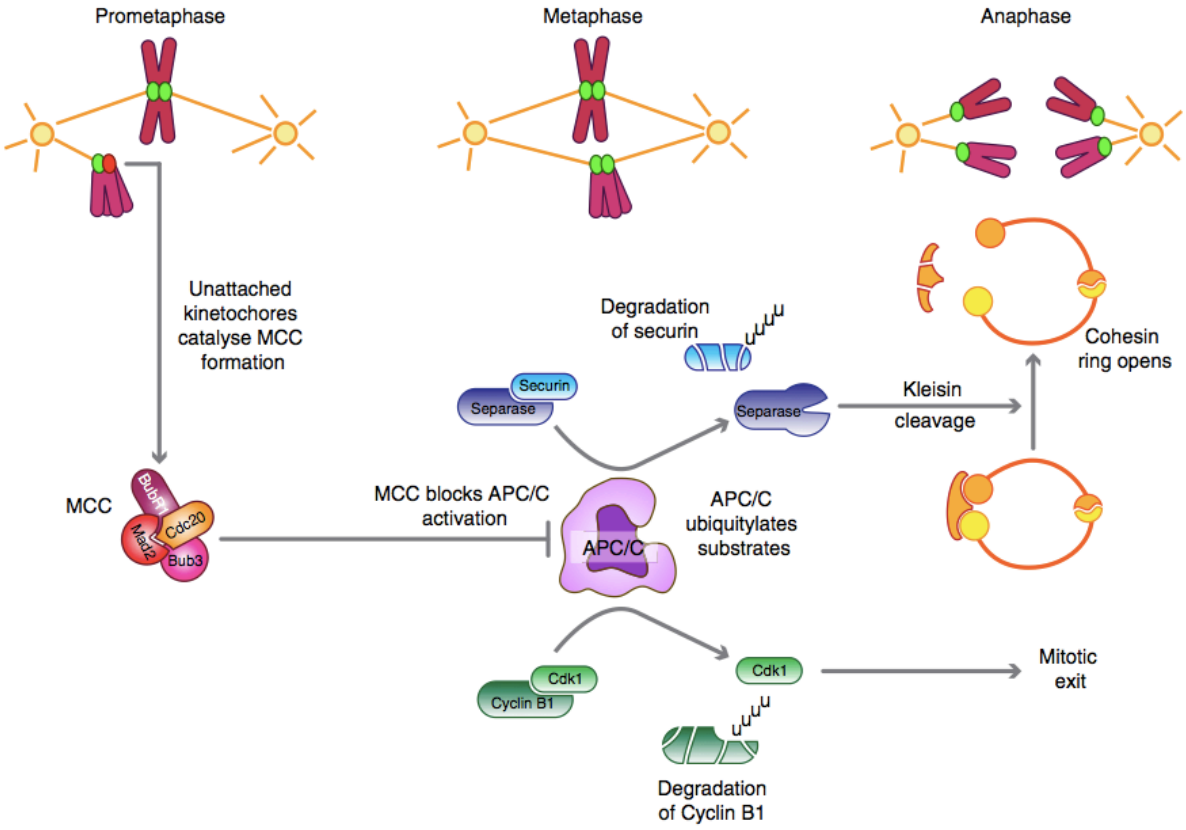

Figure 3: The spindle assembly checkpoint. The stages of spindle fibre attachment, mitotic checkpoint control (MCC) formation, and the regulation of the anaphase promoting complex/cyclosome (APC/C) through the MCC. Upon attachment of spindle fibres to the kinetochores the APC/C is activated and cyclin B1 and securin are targeted for degradation, separase becomes activated, Cohesin is cleaved and sister chromatids are separated (Lara-Gonzalez, Westhorpe & Taylor, 2012).

all chromosomes are attached to spindle and aligned on the metaphase plate, the cell cycle arrests in metaphase (Ault & Nicklas, 1989). Upon successful chromosome alignment and attachment the proteins cyclin B1 and Securin are ubiquitinated by the APC/C (anaphase promoting complex/cyclosome) and as such are targeted for degradation. The protein Separase is activated and as a consequence cleaves the Cohesin bonds between sister chromatids thus allowing the cell cycle to enter anaphase and eventually exit mitosis (Figure 3) (Clute & Pines, 1999; Bagting et al., 2002).

1.3.1 The Anaphase Promoting Complex/Cyclosome

APC/C (anaphase promoting complex/cyclosome) function is essential for normal progression through the SAC (Holloway et al., 1993). The APC/C is a highly conserved, mega-Dalton, multi-subunit, E3 ubiquitin ligase (Reviewed by Harper et al., 2002; Reviewed by Peters, 2006). It functions to regulate progression through the cell cycle by targeting cyclins and other cell cycle proteins such as Securin, for degradation by the proteasome (Irniger et al., 1995). E3 ubiquitin ligases are the final player of a multiple stage process in which proteins are targeted for degradation, and then degraded by the 26 S proteasome (Reviewed by Deshaies & Joazerio, 2009) (Figure 4). Initially ubiquitin molecules are activated, and bind to an E1 ubiquitin activating enzyme in a process that requires ATP (Reviewed by Deshaies & Joazerio, 2009) (Figure 4). Next the ubiquitin is transferred from the E1 enzyme to the ubiquitin conjugating, or E2, enzyme (Reviewed by Deshaies & Joazerio, 2009). The E2 enzyme – commonly UbcH10, or E2S in humans - then forms a complex with the APC/C and its substrate, enabling the ubiquitin molecule to be transferred to the protein substrate (Figure 4) (Jin

Figure 4: The E1, E2 and E3 Ubiquitination Pathway

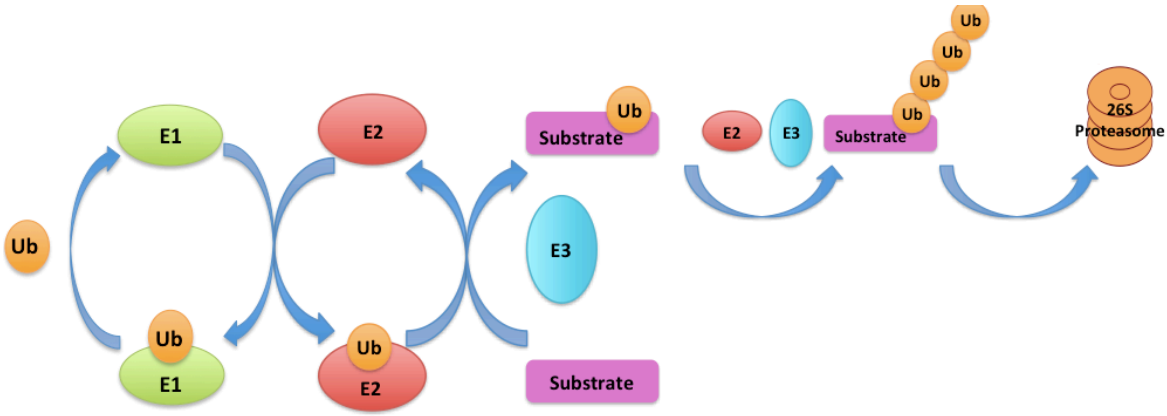

Figure 4: The E1, E2 and E3 Ubiquitination pathway. E1 ubiquitin-actvation enzyme binds to and activates ubiquitin (Ub), the Ub is then transferred to the E2 ubiquitin-conjugating enzyme. The E3 ubiquitin-ligase binds to the substrate and to the E2-Ub complex, catalysing the transfer of Ub to the substrate. This cascade of reactions continues and a Ub chain forms on the substrate. This targets the substrate for degradation by the 26S proteasome.

et al., 2008). This process continues until a ubiquitin chain forms, and finally the substrate is targeted to and degraded by the 26S proteasome (Figure 4) (Reviewed by Deshaies & Joazerio, 2009).

The APC/C has a vast range of substrates throughout many parts of the cell cycle, and requires two co-activators – Cdc20 and Cdh1 – in order to function fully (Passmore et al., 2003). These co-activators bind to the APC/C at different time points in the cell cycle and increase affinity for specific substrates, hence adding another layer of regulation to the ubiquitination

process (Passmore & Barford, 2005). This increased affinity for particular substrates is caused by the ability of Cdc20 and Cdh1 to recognise different binding sites on the substrates. Substrates for ubiquitination by the APC/C typically contain either the destruction-box (D-box) – R-X-X-L-X-X-X-X-N/D/E – or the KEN-box – K-E-N-X-X-X-D/N – motif, and some contain both (Glotzer et al., 1991; Pfleger & Kirschner 2000). Other putative motifs have been described such as the A-Box, CRY-Box and GxEN-Box (Littlepage & Ruderman, 2002; Reis et al., 2006; Castro et al., 2003). D-box motifs are typically recognised by the APC/C^{CDC20} complex while KEN-box motifs are recognised by the APC/C^{CDH1} complex (Glotzer et al., 1991; Pfleger & Kirschner 2000; Burton & Solomon, 2001). In the case of Securin at the SAC it is recognised by APC/C^{CDC20} at its D-Box, which is located between residues 61-68 (Hillioti et al., 2001; Hagting et al., 2002).

1.3.2 Separase and Securin

The ratio of Separase to Securin at metaphase is what governs the separation of the sister chromatids and therefore progression into anaphase. Separase was identified in budding yeast - *Saccharomyces cerevisiae* – as Esp1 and fission yeast – *Schizosaccharomyces pombe* – as Cut1 (Ciosk et al., 1998; Funabiki et al., 1996). It is essential for sister chromatid separation during anaphase, and was found to contain a universally conserved histidine and cysteine residues typically found in cysteine peptidases (Funabiki et al., 1996; Nasmyth, Peters & Uhlmann, 2000).

Securin homologues Pds1 and Cut2 were first identified in *S. cerevisiae* and *S. pombe* respectively (Yamammoto, Guacci & Koshland, 1996; Cohen-Fix et al., 1996). Degradation of Securin via the APC/C was also found to be essential for cell cycle progression (Funabiki et al., 1996). The human homologue of Securin was discovered in a rat growth hormone secreting pituitary cell-line and is known as PTTG (pituitary tumor-transforming gene) (Pei & Melmed, 1997).

Securin has a dual role in Separase regulation. Firstly it controls nuclear localisation of Separase (Jensen et al., 2001; Kumada et al., 2008; Zou et al., 1999; Jallepalli et al., 2001; Agarwal & Cohen-Fix, 2002). Secondly Securin binds Separase to inhibit its action upon the Cohesin complex that join sister chromatids together (Figure 3) (Coisk et al., 1998). Securin is a substrate of the APC/C^{Cdc20} ubiquitin ligase complex. Formation of the MCC (mitotic checkpoint complex) with the APC/C co-activator Cdc20 prevents the APC/C's ubiquitin ligase activity therefore preventing

degradation of Securin (Figure 3) (Sudakin et al., 2001). When all kinetochores are bound to spindle fibres the MCC is released from Cdc20, and the APC/C targets Securin for degradation by the proteasome (Figure 3) (Hagting et al., 2002). In this manner the APC/C is able to regulate the activity of Separase until the requirements of the SAC have been satisfied (Cohen-Fix et al., 1996).

1.3.3 The Mitotic Checkpoint Complex and Cdc20

The SAC is an incredibly complex system, involving many regulatory proteins and complexes. Much of the initial research into the SAC was carried out in yeast. One of the primary discoveries was the identity of the proteins which made up the MCC (mitotic checkpoint complex). The MCC is an integral part of the SAC machinery and is comprised of several components. The mitotic arrest deficient (MAD1, MAD2 and MAD3/BUBR1) and budding uninhibited by benzimidazole (BUB1) proteins which make up the MCC were first identified in budding yeast, *Saccahromyces cerevisiae* (Hoyt et al., 1991; Li & Murray, 1991). Homologues of these highly conserved proteins were later identified in humans as MAD2, BUB3 and BUBR1 (Sudakin et al., 2001). Prior to mitosis proteins are recruited to the kinetochores to form the spindle fibre attachment sites (Musacchio & Salmon, 2007). Upon entering mitosis MAD2 accumulates at unattached kinetochores in preparation for MCC formation (Musacchio & Salmon, 2007). The final component, and ultimately the target of the MCC, is the APC/C co-activator Cdc20. Cdc20 is bound by the MCC as the cells enter metaphase, inhibiting the action of the APC/C on Securin and cyclin B1 (Hwang et al., 1998; Kim et al., 1998).

The order in which the MCC forms is unknown, but it is thought that a MAD2-Cdc20 complex is required for BUB3 and BUBR1 to join the complex (Davenport, Harris & Goorha, 2006). It is also unknown whether the MCC binds Cdc20 in complex with the APC/C or in an unbound form (Fang et al., 1998). The binding of Cdc20 by the MCC prevents ubiquitination of the cyclin B1 and Securin therefore preventing progression into anaphase (Musacchio & Salmon, 2007). Upon binding of the kinetochores to the spindle fibres the MCC dissociates from Cdc20, and MAD2 levels around the kinetochores reduce 50-100 fold (Mussachio & Salmon, 2007). Following MCC dissociation from Cdc20, Securin is targeted for degradation by the APC/C, and the cell enters anaphase.

1.4 Human Securin - the Pituitary Tumor-Transforming Gene

Securin homologues Pds1 and Cut 2 were discovered in yeast in 1996 but the human form of Securin remained elusive until one year later a 202 amino acid long protein was found in a rat growth hormone secreting pituitary cell-line (Yamammoto, Guacci & Koshland, 1996; Cohen-Fix et al., 1996Pei & Melmed, 1997). This protein known as pituitary tumor-transforming gene (PTTG) was implicated in a range of cellular functions, and later found to be the human homologue of Securin (Pei & Melmed, 1997; Zou et al., 1999). After its initial discovery in a rat growth hormone secreting pituitary cell-line, PTTG was characterised in human foetal liver tissue (Pei & Melmed, 1997; Zhang et al., 1999). PTTG has since been identified as a proto-oncogene

and overexpressed in a wide range of tumours (McCabe & Gittoes, 1999; reviewed in Tfelt-Hansen, Kanuparthi & Chattopadhyay, 2006).

Aneuploidy leading to genome instability and mutation is a hallmark of cancer, and can be caused by disruption to chromosomal separation (Hanahan & Weinberg, 2011; Lengauer et al., 1998). Cahill et al. (1998), first suggested aneuploidy in colon cancers was caused by aberrant SAC activity, and this has since been confirmed in a number of other cancers. Mutations in SAC checkpoint proteins generally seem to occur in the MCC components (Cahill et al., 1998).

PTTG contributes to aneuploidy in cancer through abnormal expression levels (Chirstopoulou, Moore & Tyler-Smith, 2003). PTTG is overexpressed in a wide range of cancers including thyroid, breast, pituitary, ovarian, colorectal and lung (Heaney et al., 2000; Solbach et al., 2004; Ogbagbriel et al., 2005; Zhang et al., 1999; Puri et al., 2001; Heaney et al., 2000; Kakar & Malik, 2006). Overexpression is often associated with poor prognosis, metastasis, and reoccurrence; and has been suggested for use as a prognostic marker in multiple cancers such as thyroid, breast, pituitary, esophageal, glioma, hepatocellular carcinoma and squamous cell carcinoma of the head and neck (Boleart et al., 2003; Solback et al., 2004; McCabe et al., 2003; Shibata et al., 2002; Genkai et al., 2006; Fujii et al., 2006; Solbach et al., 2006). In recent years PTTG has been a target for anti-cancer therapies in both ovarian and lung cancer, therefore the biology behind this protein is particularly relevant for the development, and advancement of anti-cancer treatments (Yeakel & Kakar, 2008; Kakar & Malik, 2006).

1.5 PTTG Mutations

A recent study mutated most of the 32 potential phosphorylation sites of PTTG from serine, threonine and tyrosine residues to glycine or alanine (Mora-Santos et al., 2013). Of these mutants, Threonine-60-Alanine (T60A) increased PTTG half life to 30 minutes from 18, was found to cause chromosomal instability using FISH (fluorescence in-situ hybridisation), and showed increased invasiveness through matrigel invasion assay and RT-PCR (real time – polymerase chain reaction) analysis of invasion related genes (Mora-Santos et al., 2013). Until recently PTTG mutations were thought to be extremely uncommon. However there has been an increase in the number of PTTG mutations found on the COSMIC (catalogue of somatic mutations in cancer) database of late (Forbes et al., 2008; Forbes et al., 2011). One such mutation is the Threonine-60-Asparagine (T60N) residue found in a breast cancer tissue sample, which is interesting given the fuctional consequences of T60A mutation identified by Mora-Santos et al. (2013) (Stephens et al., 2012).

The Threonine 60 (T60) residue of PTTG is situated immediately adjacent to the PTTG D-Box, which occupies amino acid residues 61-69 (Figure 5) (Mora-Santos et al., 2013). In yeast Securin degradation is regulated through phosphorylation of residues adjacent to the D-Box (Holt, Krutchinsky & Morgan, 2008). Phosphorylation of the yeast Securin homologue Pds1 by the kinase Cdk1 was found to prevent ubiquitination, whereas dephosphorylation by Cdc14 promoted ubiquitination of Pds1 (Holt, Krutchinsky & Morgan, 2008). Although PTTG does not contain Cdk1 binding sites in this area phosphorylation of the T60 residue by another kinase may lead to regulation in

Figure 5: PTTG Domain Map

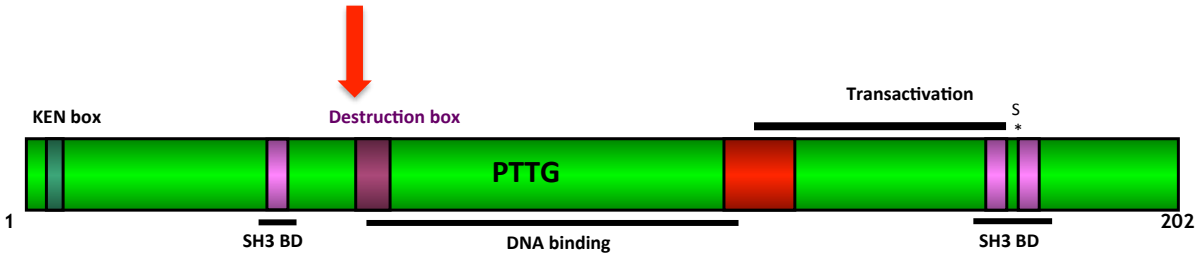

Figure 5: PTTG domain map. Location of KEN-box and D-box in PTTG. Red arrow indicates the location of the Threonine-60 residue. The D-box is located between residues 61-69.

a similar manner to Pds1 in yeast, meaning that mutation to this residue may prevent this avenue of regulation. Mutation of the residue to an amino acid with vastly different properties - from polar threonine which is able to undergo phosphorylation to polar asparagine which is bulkier than threonine and not able to undergo phosphorylation - could also interfere with enzyme-substrate interactions, or have a spatial impact on the binding site, reducing the binding ability of PTTG to the APC/C. This could potentially explain the observations made by Mora-Santos et al., 2013. This project intends to expand upon these findings and to investigate how T60 mutations may influence PTTG-APC/C interactions.

1.7 Aims and Objectives

Previous studies have suggested that mutation at the T60 residue of PTTG causes increased chromosomal instability and invasiveness. Given that this residue has also been shown to be mutated in a breast cancer we hypothesise that phosphorylation at the Threonine-60 residue modulates PTTG degradation by the APC/C in mitosis.

We aim to investigate further the contribution of residue T60 in PTTG stability and in doing so:

- Investigate interactions between WT PTTG and T60 mutants with the APC/C co-activator Cdc20 and APC/C subunit APC3
- Determine whether T60 mutants can be ubiquitinated by the APC/C
- Raise a polyclonal phospho-antibody against PTTG phosphorylated at the T60 residue

2.0 Materials and Methods

2.1 Cell Lines and Tissue Culture Conditions

2.1.1 Cell Lines

TPC1 cells were used as a model for transfection efficiency. TPC1s are a well-characterised papillary thyroid carcinoma cell line commonly used in endocrine research (Saiselet et al., 2012).

HeLa cells were used for co-immunoprecipitation, and ubiquitination assays. HeLas were isolated from cervical carcinoma cells positive for the HPV18 virus in 1952, and became the first cell-line to be established in culture (Gey et Al., 1952).

2.1.2 Tissue Culture

TPC1 cells were cultured in RPMI 1640 (Sigma) and HeLa cells in DMEM/F-12 (Gibco) both of which were supplemented with 10% (v/v) Foetal Bovine Serum (Gibco), 2 mM L-Glutamine and Penicillin and Streptomycin.

Typically cells were grown in T75 flasks and passaged once confluent. Culture medium was aspirated and cells washed gently with PBS before adding 1ml Trypsin and incubating at $37^{O}C$ for 5 minutes. After incubation 19 ml of culture medium was added, and cell density was calculated using a haemocytometer. Cells were then plated at the desired density onto new flasks.

2.2 Plasmids and Transient Transfections

2.2.1 Plasmids

A number of plasmids were used in transient transfections during this project. All constructs were inserted into the pcDNA3 (Invitrogen) vector, which was used as the vehicle only (VO) control for all transient transfections. The pcDNA3_PTTG plasmid (University of Birmingham, Birmingham, UK) was mutated to produce the mutant PTTG plasmids described below by Dr Weni Lu (University of Birmingham, Birmingham, UK), and the myc-Cdc20 and HA-APC3 plasmids were provided by Dr Andy Turnell (University of Birmingham, Birmingham UK) (Table 1).

2.2.2 Transient Transfections

TPC-1 or HeLa cells were plated onto 6-well tissue culture plates at a density of $7.5x10^4$ cells per well, or onto T25 flasks at a density of $1x10^6$ cells per well, and incubated at 37^OC overnight. The transfection reagents Fugene (Promega) and TransIT-LT1 Transfection Reagent (Mirus-Bio) were used following the manufacturers' guidelines.

Table 1: List of Plasmids

Plasmid	Construct	Supplier
pcDNA3	-	Invitrogen
pcDNA3_PTTG	PTTG	McCabe lab, University of Birmingham UK
pcDNA3_PTTG_T60N	PTTG T60N	McCabe lab, University of Birmingham UK
pcDNA3_PTTG_T60A	PTTG T60A	McCabe lab, University of Birmingham UK
pcDNA3_PTTG_T60E	PTTG T60E	McCabe lab, University of Birmingham UK
pcDNA3_Myc-Cdc20	Myc-Cdc20	Turnell lab, University of Birmingham UK
pcDNA3_HA-APC3	HA-APC3	Turnell lab, University of Birmingham UK

Table 1: List of plasmids used in all transient transfections and their suppliers.

2.2.3 Protein Harvesting

Proteins were harvested using one of three methods. Co-transfected HeLa cells for co-immunoprecipitation were harvested using NETN buffer as described below (Section 3.4.2).

Transfected TPC1 or HeLa cells were harvested from 6-well tissue culture plates using RIPA buffer (Tris-HCl (pH 7.4), 100 mM NaCl, igepal, 10% sodium deoxycholate, 100 mM EDTA) buffer, and protease inhibitor (Sigma). The medium was aspirated from the wells and washed once with 500 μl phospho-buffered saline (PBS). RIPA plus the protease inhibitor (150 μl) was added to each well and incubated at -20^{O}C for 30 minutes. The cells were then scraped using a cell scraper and transferred to a clean Eppendorf tube. Samples were sonicated on high power, for 30 seconds, twice and then centrifuged (12000 g, 10 minutes, 4^{O}C). The supernatant was then transferred to new Eppendorfs and either used immediately or stored at -20^{O}C.

2.3 Transfection and Antibody Validation

2.3.1 Sample Preparation

Harvested protein sample concentrations were calculated using a BCA Protein Assay (Thermo Scientific). A standard curve was calculated using pre-prepared BCA protein standards in the range of 0-2 mg/ml BCA. Standards and samples (4 μl) were loaded onto a 96-well plate in duplicate, to which 80 μl of the BCA Protein Assay

reagent (10:1 dilution of BCA reagent A and BCA reagent B respectively) was added. The plate was then incubated at 37^{O}C for 30 minutes, and the plate read at 562nm on a plate reader.

Samples were typically prepared for SDS-PAGE and Western Blotting analysis at a concentration of 15 mg/ml in sample buffer (10% (w/v) DTT in Laemmli Buffer (BioRad)). They were then heated at 95^{O}C for 5 minutes, and 37^{O}C for 30 minutes before being loaded onto a SDS-PAGE gel.

2.3.2 SDS-PAGE

Small glass plates were fitted together following manufacturer's guidelines. A 12% (w/v) resolving gel (10 % (v/v) acrylamide, 0.1 M Tris, 0.1 M Bicine, 0.1 % (v/v) SDS, 0.3 % (v/v) N.N.N'N' tetramethylethylenediamine-1,2-diamine (TEMED), 0.06% (w/v) ammonium persulphate (APS)) was poured in (7ml) and 3ml methanol added. Once set the methanol was poured off and a 5% stacking gel (5 % (v/v) acrylamide, 0.1 M Tris, 0.1 M Bicine, 0.1 % SDS, 0.3 % (v/v) TEMED, 0.06% (w/v) APS) added with a 12 well comb and left to set. Once set the gels were placed into the electrophoresis tank (BioRad), the reservoir filled with running buffer (0.1 M Tris, 0.1 M Glycine, 0.1% (v/v) SDS) and the combs removed. To the first well 5μl of the dual protein standard (BioRad) was added, and the samples added to the remaining wells. The tank was assembled following manufacturer's guidelines, and the samples were run at 70V for 20 minutes through the stacking gel and 140V for 1 hour through the resolving gel.

2.3.3 Western Blotting

PVDF (polyvinylidene fluoride) membrane (Millipore) was activated in 100% methanol, rinsed in distilled H_2O and washed in transfer buffer. The SDS-PAGE gel was removed from the glass plates and transferred onto a layer of sponge and filter paper in a transfer cassette before the nitrocellulose membrane was placed on top. The cassette was completed with another layer of filter paper and sponge before being placed in a transfer tank filled with transfer buffer and an ice pack. The gel was left to transfer at 360 mA for 1 hour 15 minutes.

Once transferred the membrane was removed from the tank and blocked for 1 hour at room temperature with agitation in 5% (w/v) powdered milk in TBST (0.1 % (v/v) Tween80 in Tris Buffered Saline). After blocking the membrane was washed three times in TBST (10 minutes per wash) and incubated with agitation in the appropriate primary antibody in 5% powdered milk (w/v) in TBST (Table 2) at $4^{O}C$ overnight. The membranes then underwent three more TBST washes and were incubated with agitation at room temperature with the appropriate secondary antibody in 5% powdered milk (w/v) in TBST (Table 2). Three more TBST washes were carried out. Pierce ECL (Thermo Scientific) was added to the membranes, which were then wrapped in cling film, exposed to photographic film and developed for visualisation.

Table 2: List of Anitbodies

Target	Antibody	Dilution Factor	Provider
PTTG	Monoclonal Mouse Anti-PTTG	1:1000	NeoMarker, Freemont, California, USA
T60 Phospho-PTTG	Monoclonal Rabbit Anti-Phosphorylated T60 PTTG	1:500	Covalab
Myc-(Cdc20)	Monoclonal Hybridoma Mouse Anti-Myc-(Cdc20)	1:250	Turnell Lab, University of Birmingham, UK
HA-(APC3)	Monoclonal Mouse Anti-HA-(APC3)	1:1000	Cambridge Biosciences, UK
β -Actin	Monoclonal Mouse Anti- β -Actin	1:10000	Sigma-Aldrich
Mouse IgG	Polyclonal Rabbit Anti-Mouse HRP	1:2000	Dako
Rabbit IgG	Polyclonal Goat Anti-Rabbit HRP	1:2000	Dako

Table 2: List of primary and secondary antibodies used in Western Blotting including dilution factors and providers.

2.4 Co-Immunoprecipitation

2.4.1 Cell Synchronisation

HeLa cells were transfected with the appropriate plasmids and incubated at 37^{O}C for 24 hours. Nocodazole (0.4 mg/ml in DMSO) was prepared at a concentration of 400 ng/ml in culture medium; 1 ml of this mix was added per T75 flask used. Cells were then incubated for 16 hours at 37^{O}C.

After 16 hours the cells underwent mitotic shake-off and were centrifuged (1200 rcf, 5 minutes, 4^{O}C). The supernatant was aspirated, and the pellets washed twice in culture medium (5 ml). The pellets were then re-suspended in culture medium plus 5 μM MG132 (from a 20 μM Mg132 stock), plated onto T25 flasks and incubated for 2 hours at 37^{O}C.

2.4.2 Protein Harvesting and Co-Immunoprecipitation

Once cell synchronisation was complete the cells were washed twice with ice-cold saline, and re-suspended in 900 μl NETN buffer (20 mM Tris (pH 7.5), 250 mM NaCl, 25 mM NaF, 25 mM β-glycerophosphate, 1 mM EDTA (pH 8.0), 1% (v/v) Nonidet P-40) on ice for 30 minutes with agitation.

The cells in the NETN buffer were then transferred to a tight dounce hand homogeniser for lysis, and each sample was homogenised with 15 strokes. Samples

were then transferred to a new Eppendorf and centrifuged (13000 rpm, 5 minutes, 4^{O}C). The supernatant was transferred to a new Eppendorf using a syringe, taking care not to disturb the lipid layer. At this point 25 μl of the lysate was retained for each sample and stored at -20^{O}C. The samples were then incubated rotating overnight at 4^{O}C with a monoclonal mouse hybridoma anti-myc-(Cdc20) antibody (Turnell Lab, University of Birmingham, Birmingham, UK) a 1:250 dilution.

Protein G Sepharose beads (50 μl, GE Healthcare) were added to each sample and incubated, rotating, at 4^{O}C for a further 2 hours. The samples were centrifuged at (13000 rpm, 1 minute, 4^{O}C) to pellet the Protein G beads and the supernatant removed. The beads were washed in NETN (500 μl) 5-7 times, and the final wash aspirated using a syringe. To each sample 30 μl of sample buffer (10% (v/v) SDS, 9 M Urea, 50 mM Tris (pH 7.4), 100 mM β -mercaptoethanol) was added, and 25 μl sample buffer added to the cell lysate samples retained previously, in preparation for SDS-PAGE and Western blotting.

2.4.3 SDS-PAGE and Western Blotting

Co-immunoprecipitation (Co-IP), ubiquitination assay (section 3.5.2) and GST-pull down (section 3.5.3) samples were all separated by SDS-PAGE on large acrylamide gels using the following protocol.

Typically samples were loaded onto a 10% resolving gel (10 % (v/v) acrylamide, 0.1 M Tris, 0.1 M Bicine, 0.1 % SDS, 0.3 % (v/v) TEMED, 0.06% (w/v)

APS) with a protein ladder (Made in House). The electrophoresis tank was then assembled according to manufacturer's guidelines, and running buffer (0.1 M Tris, 0.1 M Bicine, 0.1% (v/v) SDS) poured into the reservoir. The samples were then run at continuous voltage of 18 V overnight

Co-IP samples were then further analysed by established Western blotting techniques. The SDS-PAGE equipment was dismantled and the gel cut down to the appropriate size. Nitrocellulose membrane (PALL) was activated in transfer buffer (25 M Tris, 192 mM glycine, 20% (v/v) methanol) and the Western blotting equipment assembled according to manufacturer's guidelines. The transfer was then run at 280 mA for 5 hours.

Membranes were washed once in TBST before blocking in 5% powdered milk (w/v) in TBST for 1 hour at room temperature. The Monoclonal Rabbit Anti-PTTG primary antibody (NeoMarker, Freemont, California, USA) was made at a 1:1000 dilution factor in 5% powdered milk (w/v) in TBST and incubated with the membrane at $4^{O}C$ with agitation overnight. Membranes were washed for 10 minutes in TBST three times, before incubation at room temperature for 1 hour in Protein G-HRP (BioRad) at a 1:2000 dilution in 5% powdered milk (w/v) in TBST. After the final incubation membranes were washed three times in TBST for 10 minutes each. Pierce ECL (Thermo Scientific) was made up according to manufacturer's guidelines and added to the membranes before wrapping in cling film. Blots were visualised by exposure to photographic film for the optimum exposure time, which were then developed using the X-OGraph Developer.

2.5 *In vitro* Studies

2.5.1 L-α-[^{35}S]-Methionine Radiolabelled in vitro Protein Synthesis

Radiolabelled *in vitro* protein constructs of PTTG, PTTG T60N, PTTG T60A and PTTG T60E proteins were prepared using the appropriate plasmids, L-α-[^{35}S]-methionine (500μCi, Perkin Elmer) and a TNT T7-Coupled Rabbit Reticulocyte Lysate System (Promega) for coupled treanscription-translation following the manufacturer's instructions.

2.5.2 Ubiquitination Assay

HeLa cells in T75 flasks were synchronised as described in section 3.4.1, and after undergoing mitotic shake-off were centrifuged (14000 rpm, 5 minutes). The supernatant was removed, and the cell pellet washed twice with culture media. Upon completion of the second wash the pellet was re-suspended in 10 mls of culture medium and incubated at 37^{O}C for 1 hour.

After incubation the cells were placed on ice, washed twice in ice-cold isotonic saline, and re-suspended in 12 ml APC/C lysis buffer (20 mM Tris (pH7.5), 100 mM NaCl, 20 mM β -glycerophosphate, 5 mM $MgCl_2$, 0.2% (v/v) NP-40, 10% (v/v) glycerol, 1 mM NaF, 0.5 mM DTT) and left to stand for 5 minutes at 4^{O}C. Cells were

then lysed using 15 strokes of a tight dounce homogeniser, waiting for 5 minutes, and repeating. The lysate was then centrifuged at 13200 rpm for 20 minutes at $4^{O}C$.

The supernatant of the lysate was removed using a syringe, taking care not to remove the lipid layer, and divided equally between Eppendorfs so that for each ubiquitination assay there were two Eppendorfs of lysate, one positive and one negative. To each positive lysate Eppendorf the anti-APC3 antibody AF3.1 was added, and all lysate samples were incubated, rotating overnight at $4^{O}C$.

Protein-G Sepharose beads (Sigma) were re-suspended in the APC/C lysate buffer at a 1:1 ratio; 20 μl equivalent of packed beads was added to each sample and was incubated, rotating at $4^{O}C$, for 2 hours. Samples were then washed in APC/C lysate buffer once, and a high salt buffer (BL) twice. To each sample 20 μl ubiquitination assay mix (5 mM $MgCl_2$, 5 mM ATP, 10 mM creatine phosphatase, 350 Um^{-1} CPK, 1.25 mg/ml ubiquitin, 20 μg/ml ubiquitin aldehyde, 50 μg/ml E1 [his-tagged recombinant hUB1], 40 μg/ml E2 [his-tagged recombinant UBch10 and UBE2S], in BL buffer) and 1 μl of the L-α-[^{35}S]-methionine labelled proteins was added and incubated in a water bath at $37^{O}C$ for 1 hour. Upon completion of the incubation SDS-PAGE sample buffer was added and samples separated by SDS-PAGE (as described in section 3.4.3). The acrylamide gel was then dried, and visualised by autoradiography.

2.5.3 GST-Pulldown Assay

The *in vitro* translated L-α-[^{35}S]-methionine radiolabelled proteins (10 μl) were incubated with either GST-APC3 or GST-Cdc20 fusion proteins (10 μg) at 4^{O}C for 1 hour. Reaction volumes were then equalised by the addition of GST lysis buffer (1% (v/v) Triton X-100, 1mM EDTA (pH 8.0) in PBS). Packed glutathionine-agarose beads (Sigma) (20 μl) were added and the samples were incubated, rotating at 4^{O}C for 1 hour.

Following the incubation period the samples were washed three times with GST lysis buffer and a further two times with GST wash buffer (1mM EDTA (pH 8.0) in PBS). Samples were eluted from the glutathionine-agarose beads with GST elution buffer (25 mM reduced glutathione in 50 mM Tris (pH 8.0)) and SDS-PAGE sample buffer (10% (v/v) SDS, 9 M Urea, 50 mM Tris (pH 7.4), 100 mM β -mercaptoethanol) added. Samples were then separated by SDS-PAGE (as described in section 3.4.3), the acrylamide gel dried, and then visualised by autoradiography.

3.0 Results

3.1 Expression of PTTG mutants in TPC1 Cells

Initially we assessed the transfection efficiency of the PTTG expression plasmids established in TPC1 cells (Figure 6). Wild type PTTG and the PTTG mutants were all successfully transfected and gave bands of the expected size (Figure 6). Myc-Cdc20 was also successfully transfected to similar levels. However, transfection of the HA-APC3 plasmid was unsuccessful. Due to the time constraints of the project it was decided that analysis of APC3 interactions with WT (wild type) PTTG and PTTG mutants would not be explored by Co-IP.

3.2 Investigating the interaction between PTTG mutants and Cdc20

In order to investigate potential interactions between the WT and mutant PTTG proteins and Cdc20, HeLa cells were co-transfected with each of the PTTG plasmids and the myc-Cdc20 plasmid. Complexes were pulled-down with a monoclonal mouse hybridoma anti-myc antibody, and detected using the monoclonal mouse anti-PTTG primary antibody. Data collected from a preliminary Co-IP experiment used asynchronous cells and vehicle only transfected with myc-Cdc20 as a control (Figure 7). Data suggested that WT PTTG and the PTTG mutants T60N, T60A and T60E interacted with with myc-Cdc20 to varying degrees, with interaction decreased in wild type PTTG compared to that seen in the mutants (Figure 7).

Figure 6: Transfection of WT and Mutant PTTG in TPC1 Cells

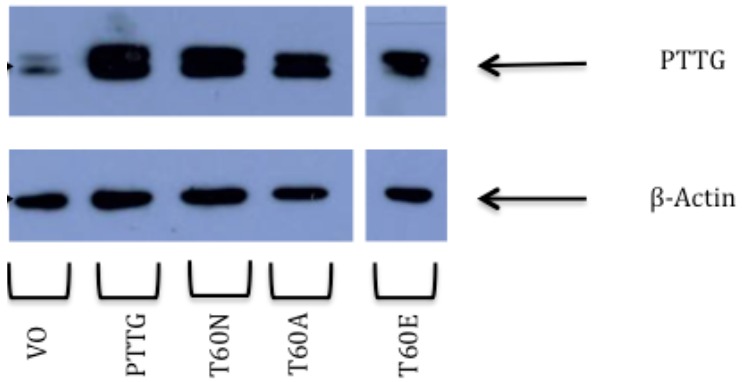

Figure 6: Transfection of WT and mutant PTTG in TPC1 cells. Transfection test of the PTTG plasmids expressing WT PTTG, PTTG T60N, PTTG T60A and PTTG T60E. All proteins were transfected successfully and expressed at levels higher than that of endogenous PTTG observed in the VO (Vehicle Only) transfection.

Figure 7: Preliminary myc-Cdc20-PTTG Co-IP in Asynchronous HeLa Cells

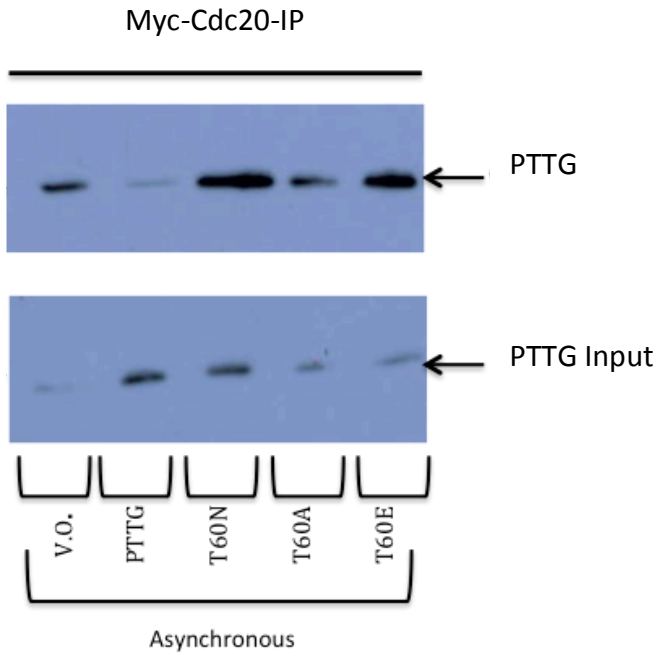

Figure 7: Preliminary myc-Cdc20-PTTG Co-IP in asynchronous HeLa cells. Protein complexes were pulled down with a monoclonal mouse hybridoma anti-myc-Cdc20 antibody and detected using a monoclonal mouse anti-PTTG primary antibody. The blot indicates that all of the PTTG proteins are able to interact with myc-Cdc20, with increased intensity in the T60N and T60E lanes. Interaction between PTTG and Cdc20 appears to be decreased in the WT PTTG lane.

Figure 8: Replicate myc-Cdc20-PTTG Co-IP in Synchronised HeLa Cells

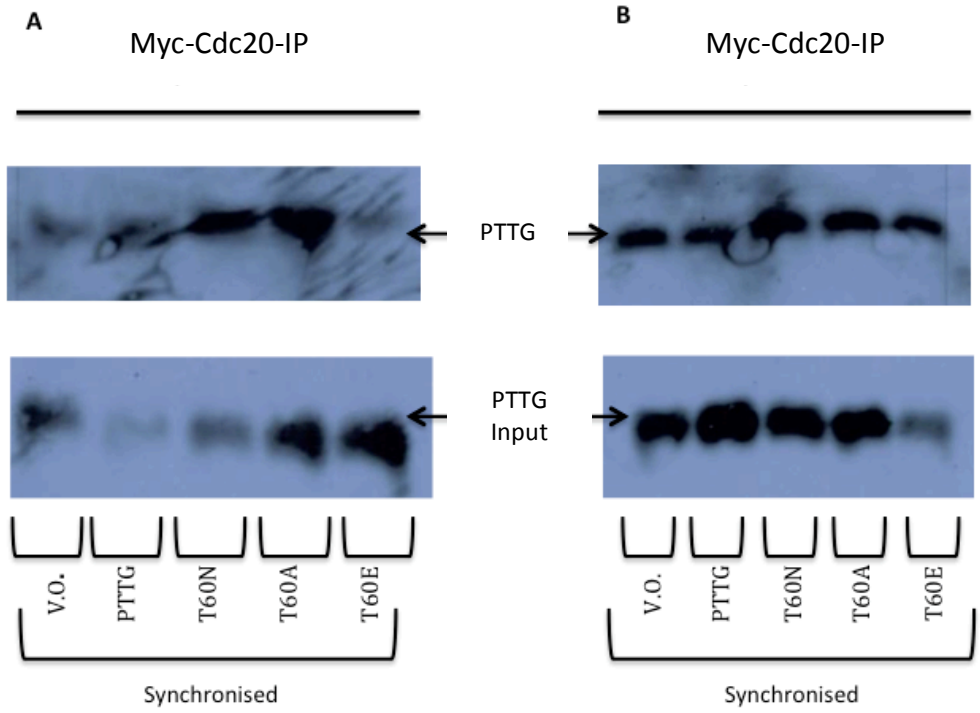

Figure 8: Replicate myc-Cdc20-PTTG Co-IP in synchronised HeLa cells. Protein complexes were pulled down with a monoclonal mouse hybridoma anti-myc-Cdc20 antibody and detected using a monoclonal mouse anti-PTTG primary antibody. (A) The first repeat in synchronised cells indicates that all of the PTTG proteins interact with myc-Cdc20, with increased intensity in the T60N and T60A lanes and decreased interaction in the PTTG and T60E lane. (B) The second repeat in synchronised cells suggests that all proteins are able to interact with myc-Cdc20 at similar levels, with perhaps a slight increase in T60E.

The Co-IP was repeated twice more using synchronised cells. Nocadazole release was used to achieve synchronisation of cells during mitosis and optimise the amount of transfected myc-Cdc20 associated with the APC/C. Results differed between the two repeats, with one showing a similar trend to that seen in the asynchronous cells (Figure 8 A), and the other indicative of PTTG mutants T60N, T60E and T60A being able to bind to myc-Cdc20 at similar levels observed for normal PTTG (Figure 8 B).

To assess these interactions in more detail, more appropriate controls need to be performed. Ideally the Co-IPs would have been run with samples incubated with and without the myc-Cdc20 antibody in order to highlight any non-specific binding. To further investigate the relationship between the PTTG mutants and the APC/C *in vitro* ubiquitination and GST-pulldown studies were carried out to investigate whether these mutants were substrates for the APC/C or interacted APC/C components.

3.3 PTTG Mutants are Substrates for APC/C-Directed Ubiquitin Ligase Activity

To broaden our understanding of the interaction between the PTTG mutants with Cdc20, as suggested by the preliminary Co-IP data, the PTTG plasmids were used to synthesise *in vitro* L-α-[^{35}S]-methionine radiolabelled proteins. The capacity of these radiolabelled proteins to undergo APC/C-directed ubiquitination was tested. To do this, the entire APC/C was precipitated from HeLa cells by immunoprecipitation with the AF3.1 APC3 antibody radiolabelled proteins were added to a mix containing E1, and E2 enzymes along with all the other essential components required for ubiquitination to

Figure 9: Ubiquitination of APC/C Substrates Cyclin A and Cyclin B

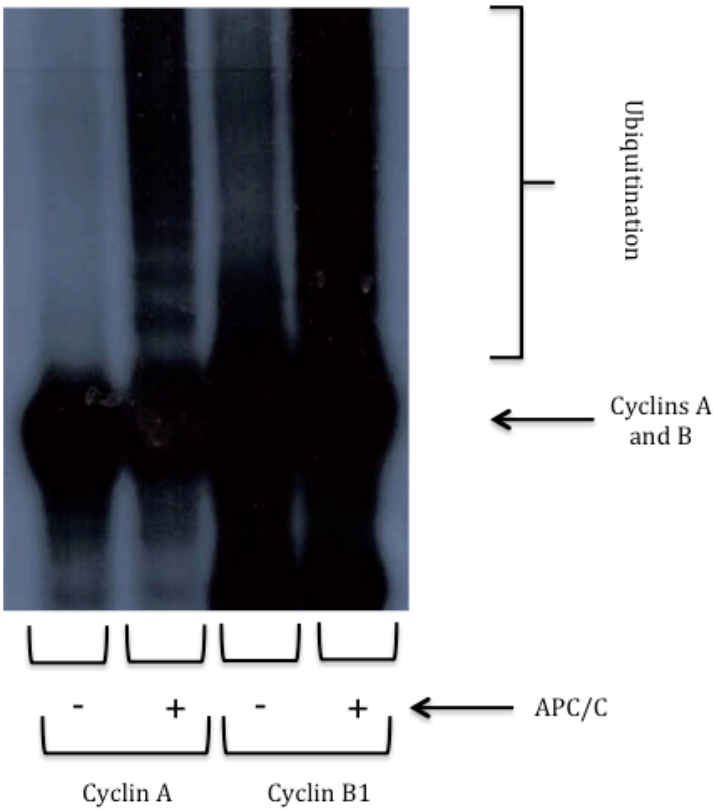

Figure 9: Ubiquitination of APC/C substrates cyclin A and cyclin B Ubiquitination assay of L-α-[^{35}S]-methionine radiolabelled known APC/C substrates cyclin A and cyclin B. The negative (-) and positive (+) markers indicate the absence and presence of the APC/C respectively. Ubiquitination of both cyclin A and cyclin B can be clearly seen in the positive lanes of the gel.

Figure 10: Ubiquitination of WT PTTG and Mutant PTTG

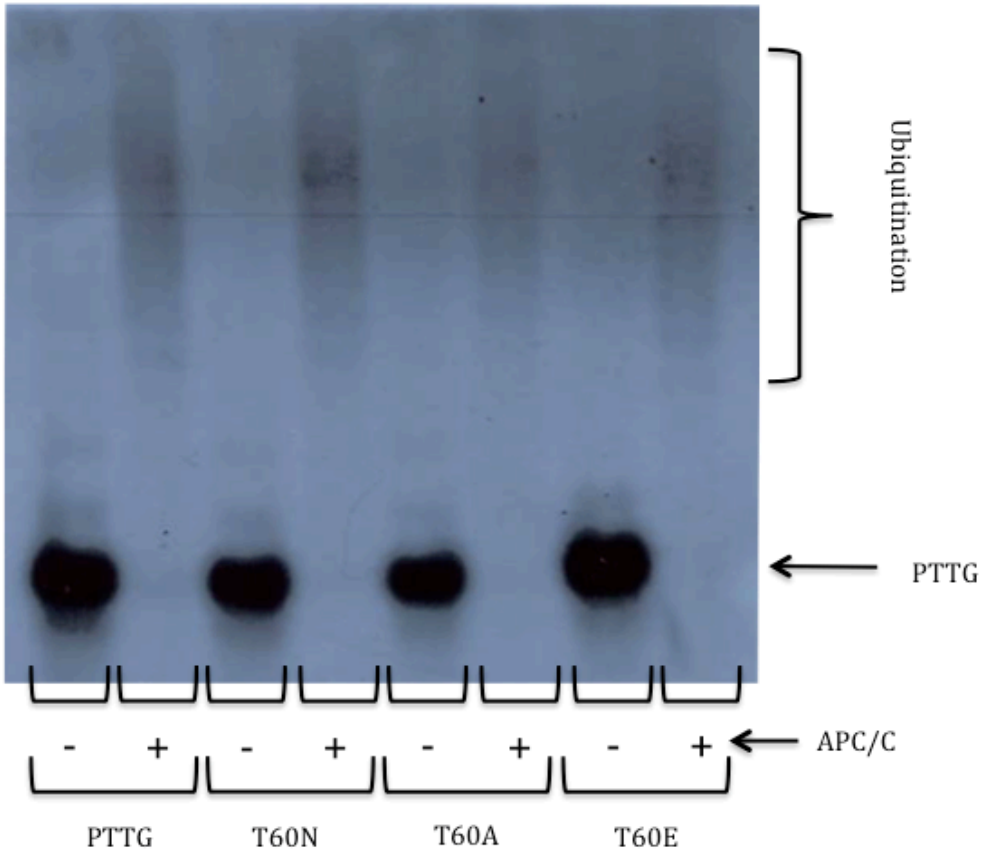

Figure 10: Ubiquitination of WT PTTG and mutant PTTG. Ubiquitination assay of [^{35}S]-Methionine radiolabelled WT PTTG, PTTG T60N, PTTG T60A and PTTG T60E proteins. The negative (-) and positive (+) markers indicate the absence and presence of the APC/C respectively. Ubiquitination of all PTTG forms can be seen.

take place. The assay took place with and without the presence of the APC/C to have positive and negative controls respectively, thus enabling the ubiquitination status of the proteins to be established.

To further validate results radiolabelled Cyclin A and Cyclin B1 - known APC/C substrates – were used in the assay as positive controls to demonstrate successful ubiquitination (Figure 9). The assay was repeated twice with the *in vitro* translated PTTG and PTTG mutants (Figure 10). The results from both assays are indicative of ubiquitination of PTTG, PTTG_T60N, PTTG_T60A and PTTG_T60E, and indicates that they are all viable substrates for the APC/C^{Cdc20}.

3.4 Investigating the Interaction of the PTTG mutants and APC/C Subunits *in vitro*

The radiolabelled *in vitro* produced PTTG proteins were also used in GST pulldown experiments. Both Cdc20 and APC3 were available as GST tagged proteins providing an *in vitro* alternative to Co-IP experiments. This was a particularly useful tool for the evaluation of APC3 interactions with the different PTTG forms, as the plasmid expressing HA-APC3 was not successfully transfected for Co-IP studies to be carried out.

Preliminary findings indicated some interaction between the PTTG proteins with both GST-Cdc20 and GST-APC3 (Figure 11 B and C). The intensity of the bands varied

Figure 11: GST-Pulldown Assay of GST-APC3 and GST-Cdc20 with PTTG

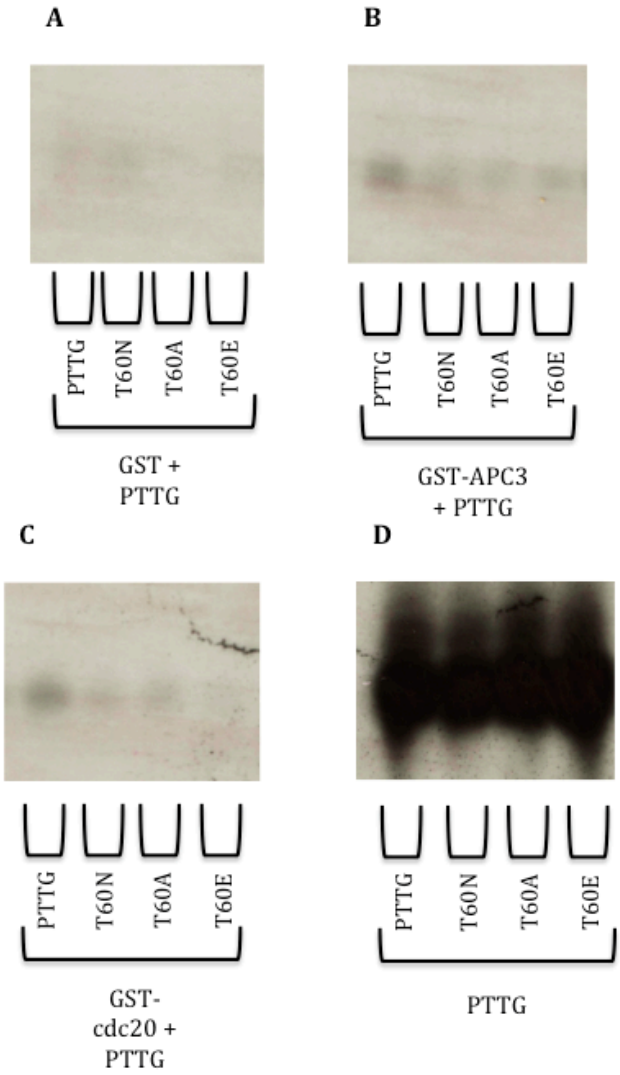

Figure 11: GST-pulldown assay of GST-APC3 and GST-Cdc20 with PTTG. (A) the PTTG proteins were incubated with GST alone (B) the PTTG proteins were incubated with GST-tagged APC3 (C) the PTTG proteins were incubated with GST-Cdc20 (D) indicates the starting levels of PTTG in each assay.

between PTTG forms, suggesting a higher interaction between wild type PTTG and the GST-APC3 and GST-Cdc20 proteins compared to that seen in the PTTG mutants T60N, T60A and T60E (Figure11 B and C). Non-specific interactions between the PTTG proteins and the GST tag were ruled out through incubation with the GST tag alone (Figure 11 A). The exposure time for the autoradiography was 120 hours (5 days) meaning that the intensity of the result were much lower levels than the starting amount of PTTG proteins (Figure 11 D), and perhaps if time constraints had allowed the assay would have been repeated to optimise the protocol.

3.5 Antibody Validation

During the course of this project we initiated the construction of a phospho-specifc antibody to the phosphorylated form of the T60 residue in PTTG. This was carried out by Covalab over a course of 109 days using two female New Zealand white rabbits (rabbits 1223046 and 1223049 respectively). Three peptides were designed for use in the immunisation protocol in order to optimise the specificity of the antibodies being generated; a control peptide specific to the region surrounding the T60 residue in PTTG (FDAPPALPKATRKAL), a long phospho-peptide (FDAPPALPKA**Tp**RKAL) and a short phosphor-peptide (LPKA**Tp**RKA).

A bleed was taken from each rabbit on day 0 followed by immunisation with the control PTTG peptide. Injection with the long phospho-peptide was repeated on day 21,

Figure 12: Validation of Day 53 Polyclonal T60 Phospho-Specific Antibody Bleed

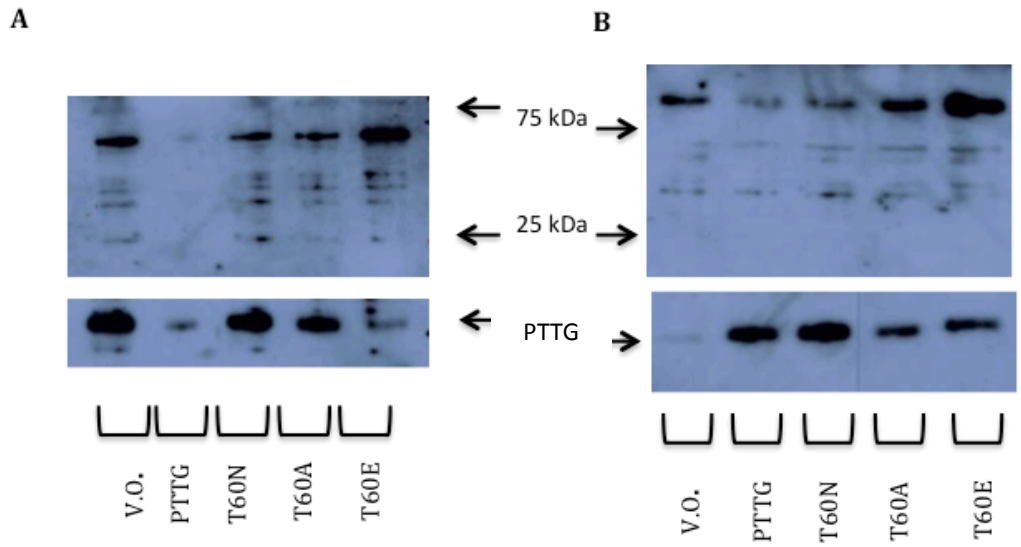

Figure 12: Validation of day 53 polyclonal rabbit T60 phospho-specific antibody bleed. Antibody validation in HeLa cells using the day 53 bleeds membranes probed initially with the bleeds followed by re-probing with the Monoclonal Mouse Anti-PTTG antibody (A) Rabbit 1223046 day 53 bleed, with some binding seen at the 25 kDa marker correlating to where PTTG runs on a gel. (B) Rabbit 1223049 day 53 bleed, little to no binding seen at the 25 kDa marker. Both (A) and (B) show non-specific binding to a number of proteins.

Figure 13: Validation of Day 88 Polyclonal T60 Phospho-Specific Antibody Bleed

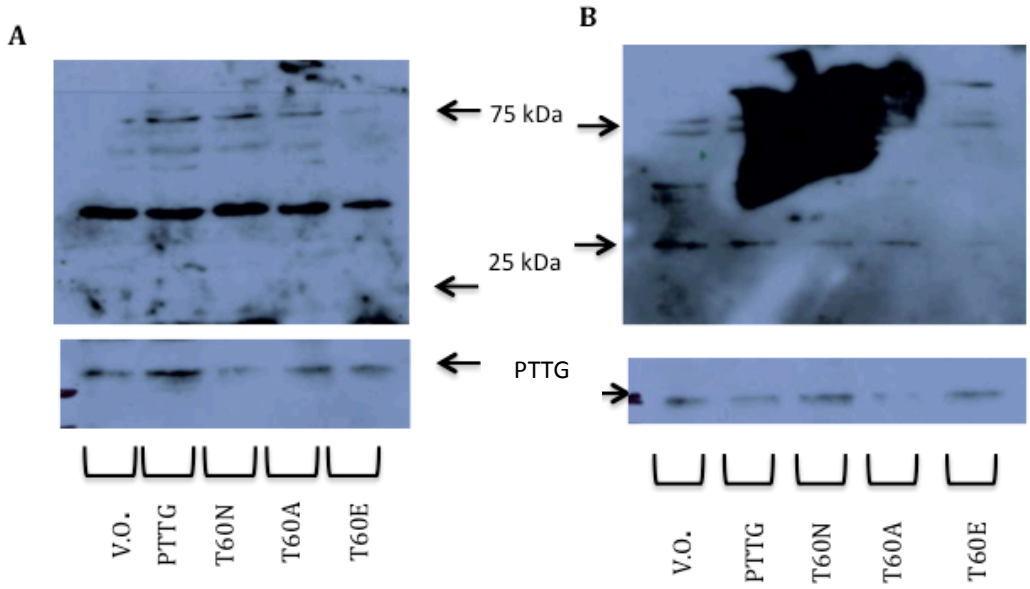

Figure 13: Validation of day 88 polyclonal rabbit T60 phospho-specific antibody bleed. Antibody validation in HeLa cells using the day 88 bleeds membranes probed initially with the bleeds followed by re-probing with the Monoclonal Mouse Anti-PTTG antibody (A) Rabbit 1223046 day 88 bleed, with little to no binding seen at the 25 kDa marker correlating to where PTTG runs on a gel. (B) Rabbit 1223049 day 88 bleed, some binding seen at the 25 kDa marker correlating to where PTTG runs on the membrane. Both (A) and (B) show non-specific binding to a number of proteins.

and the first injection with the short phospho-peptide was performed on day 42. The first test bleed was taken from each rabbit on day 53. Two more injections of the short phospho-peptides were carried out on days 63 and 77 before a second test bleed was taken on day 88. Specificity of the antibodies in the bleeds was tested on the transfected proteins PTTG, PTTG T60N, PTTG T60A, and PTTG T60E. (Figures 12 and 13 respectively).

The specificity between the day 53 bleeds from the two rabbits varied. Both bleeds bound to several non-specific proteins (Figure 12). However, Rabbit 1223046 showed some specificity for PTTG along the 25 kDa marker point, but not specificity for the phosphorylatable form of PTTG as binding was observed across all PTTG proteins (Figure 12 A). Little to no binding at the 25 kDa marker was observed with the 1223049 bleed, compared to that by the PTTG antibody at this time point (Figure 12 B).

The day 88 bleeds brought further variation to the previous findings. Whereas with the day 53 bleeds the most specificity for PTTG was observed in 1223046 the opposite was seen for the day 88 bleeds, with more specificity in 1223049 (Figure 13 B). Again there was no real distinction between the phosphorylatable form of PTTG and the PTTG mutants T60N, T60A and T60E (Figure 13). Therefore two bleeds had low avidity for T60 phosphorylated-PTTG, or very low levels of T60 phosphorylated-PTTG. Due to these findings, it was determined that an extension of the immunisation protocol from 109 days to123 days would optimise the development of this phospho-specific antibody.

4.0 Discussion

PTTG over expression has been well catalogued in a number of cancers, however investigation into incidences of PTTG mutations in cancer has been explored very little (Heaney et al., 2000; Solbach et al., 2004; Ogbagbriel et al., 2005; Zhang et al., 1999; Puri et al., 2001; Heaney et al., 2000; Kakar & Malik, 2006). This project aimed to examine the effect of PTTG mutation at the T60 residue, following on from the recently published research by Mora-Santos et al. (2013) and hypothesised that phosphorylation at the Threonine-60 residue modulates PTTG degradation in mitosis. Co-IP studies evaluating interactions between myc-Cdc20, WT PTTG and the mutant PTTG forms suggested WT PTTG bound less strongly to myc-Cdc20 than the PTTG mutants. Ubiquitination assays demonstrated that the PTTG mutants were ubiquitinated to the same extent observed for WT PTTG, and a preliminary GST-assay indicated that the PTTG forms may interact with both Cdc20 and APC3. These findings indicate that mutations to the T60 residue is unlikely to regulate PTTG interaction with the APC/C in a negative manner.

The reduced binding of WT PTTG to myc-Cdc20 observed in the Co-IP experiments correlates with methods employed in the regulation of APC/C binding with other mitotic substrates. For example Cdc6 is a protein targeted for degradation by the APC/C early in the cell cycle (at G1 phase) to prevent pre-replicative complexes forming prior to S phase (Peterson et al., 2000). At the onset of S phase Cdc6 undergoes phosphorylation by the Cyclin E-Cdk2 complex, preventing the APC/C binding and therefore preventing degradation (Mailand & Diffley, 2005). In yeast a similar

regulatory mechanism is seen in the Securin homologue Pds1, whereby phosphorylation by Cdk1 resuces APC/C interactions, stabilising Pds1, therefore suggesting that such a mechanism in the human Securin homologue PTTG may not be so far-fetched (Holt, Krutchinsky & Morgan, 2008).

PTTG has one well established phosphorylation site at the Serine-165 residue (Ramos-Morales et al., 2000). Phosphorylation of this site is known to confer changes in PTTG activity (Boelaert et al., 2004). Although there are no known kinase concensus motifs in the region surrounding the T60 residue there are examples of regulation of other mitotic proteins through phosphorylation of non-consensus motifs by kinases (Mora-Santos et al., 2013; Colgan et al., 1998; Shah, Ghosh & Hunter, 2003). For example, Poly (A) Polymerase is regulated by cyclin B/Cdk1 at both consensus and non-consensus sites, as is Ribosomal S6 Kinase 1which is regulated by Cdk1 (Colgan et al., 1998; Shah, Ghosh & Hunter, 2003).

The results from this project have been slightly contradictory in so far as expecting that T60 PTTG mutations might lead to decreased APC/C interaction and hence increase stability of PTTG. The ubiquitination assay showed WT PTTG and the PTTG mutants were all readily ubiquitinated by the immunoprecipitated APC/C. Therefore this contradicts the increased stability of the T60A mutant compared to WT PTTG observed by Mora-Santos et al. (2013). However, along with PTTG over-expression being a cause of abnormal cell division low expression levels of PTTG can also result in abnormal cell division; therefore the potentially increased affinity of the

mutant T60 PTTG proteins could result in similar effects as seen in cells with reduced PTTG expression levels (Yu et al., 2000).

The increased stability observed by Mora-Santos et al. (2013) may be related to reduced binding of another E3 ubiquitin ligase. The SCF E3 ubiquitin ligase has been found to degrade phosphorylated PTTG (Gil-Bernabé et al., 2006). Gil-Bernabé et al. (2006) found that PTTG was a substrate for protein phosphatase 2A(PP2A), and that dephosphorylation of PTTG by PP2A induced stablility. The de-phosphorylation prevented ubiquitination of PTTG by the SCF E3 ligase in all stages of the cell cycle, independently of APC/C, therefore preventing it from being targeted for degradation by the 26S proteasome (Gil-Bernabé et al., 2006). This could explain the discrepancies between the results in this project and those observed by Mora-Santos et al. (2013) and warrants further investigation.

To further investigate these findings and to establish the contradictory results of this study and of Mora-Santos et al. (2013) a stability assay looking at PTTG levels over a time course at the SAC would need to be carried out. Mora-Santos et al. (2013) indicated that the T60A mutation led to increased half-life compared to that of WT PTTG. However, this was carried out in asynchronous cells where the APC/C complex would have been in complex with both Cdh1 and Cdc20. A stability assay in cells treated with nocodazole to halt cells at the metaphase to anaphase transition would ensure that the APC/C was in complex with Cdc20, and therefore provide a more accurate insight into stability of the PTTG mutants compared to that of WT PTTG. Co-

IP experiments to investigate interaction of WT PTTG and the mutant PTTG proteins with PP2A or the SCF E3 ubiquitin ligase would also be of interest.

Although the Co-IP experiments suggest that WT PTTG binds less strongly to myc-Cdc20 than the PTTG mutants, the experiment needs to be optimised and more repeats carried out. Negative controls, where the Co-IP is carried out without the myc-Cdc20 antibody, need to occur simultaneously with those incubated with the myc-Cdc20 to rule out non-specific binding. The findings of the GST-Assay oppose the Co-IP results, suggesting that WT PTTG binds more strongly to Cdc20 and APC3 than the PTTG mutants. This could be influenced by the proteins having been synthesised *in vitro* and thus not being in a phosphorylated form for the assay. The GST-assay was a preliminary study and therefore requires optimisation and repetition before more solid conclusions can be drawn from the data. Finally once the phospho specific PTTTG antibody has been fully developed and purified, it could be utilised to screen a wide range of primary tissue samples, and types of tissue samples to look incidences of T60 mutational status in cancer.

5.0 References

Agarwal R and Cohen-Fix O (2002) Phosphorylation of the mitotic regulator Pds1/securing by cdc28 is required for effiecient nuclear localisation of Esp1/separase. *Genes Dev.,* **16** 1371-1382

Ault JG an Nicklas RB (1989) Tension, microtubule rearrangements, and the proper distribution of chromosomes in mitosis. *Chromosome*, **98** (1) 33-39

Boelaert K, Yu R, Tannahill LA, Stratford AL, Khanim FL, Eggo MC, Moore JS, Young LS, Gittoes NJL, Franklyn JA, Melmed S and McCabe CJ (2004) PTTG's C-terminal PXXP motifs modulate critical cellular processes *in vitro*. *J Mol Endocrinol*, **33** 633-677

Boleart K, McCabe C, Tannahill L, Gittoes N, Holder R, Watkinson J, Bradwell A, Sheppard M and Franklyn J (2003) Pituitary tumour transforming gene and fibroblast growth factor-2 expression: potential prognostic indicators in differential thyroid cancer. *J Clin Endocr Metab*, **88** 2341-2347

Boveri T (1914) Zur frage der entstehung maligner tumoren

Burton JL and Solomon MJ (2001) D box and KEN box motifs in budding yeast Hsl1p are required for APC-mediated degradation and direct binding to Cdc20p and Cdh1p. *Genes & Development,* **15** (18) 2381-2395

Cahill DP, Lengauer C, Yu J, Riggins GJ, Willson JK, Markowitz SD, Kinzler KW and Vogelstein B (1998) Mutations of mitotic checkpoint genes in human cancers. *Nature Letters*, **349** 300-303

Castro A, Vigneron S, Bernis C, Labbe JC and Lorca T (2003) Xkid is degraded in a D-box, KEN-box and A-box-independent pathway. *Mol Cell Biol,* **23** 4126-4138

Ciosk R, Zachariae W, Michaelis C, Shevchenko A, Mann M, and Nasmyth K (1998) An Esp1/Pds1 complex regulates loss of sister chromatid cohesion at the metaphase to anaphase transition in yeast. *Cell*, **93** (6) 1067-1076

Clute P and Pines J (1999) Temporal and spatial control of cyclin B1 destruction in metaphase. *Nature Cell Biol.* **1** 82-87

Cohen-Fix O, Peters JM, Kirschner MW and Koshland D (1996) Anaphase intiation in *Saccharomyces cerevisiae* is controlled by the APC-dependent degradation of the anaphase inhibitor Pds1p. *Genes & Development*, **10** 3081-3093

Colgan DF, Murthy KG, Zhao W, Prives C and Manley JL (1998) Inhibition of poly (A) polymerase requires p34cdc2/cyclin B phosphorylation of multiple concensus and non-concensus sites. *EMBO*, **17** (4) 1053-1062

Davenport J, Harris LD and Goorha R (2006) Spindle checkpoint function requires Mad2 dependent Cdc20 binding to the Mad3 homology domain of BubR1. *Exp. Cell Res.* **312** 1831-1842

Deshaies RJ and Joazerio AP (2009) RING domain E3 ubiquitin ligases. *Annu Rev Biochem*, **78** 399-434

Dominguez A, Romos-Morales F, Romero F, Rios R, Dreyfus F, Tortolero M and Pintor-Toro J (1998) hpttg, a human homologue of rat pttg is overexpressed in haemopoetic neoplasms. *Oncogene*, **17** 2187-2193

Evans T, Rosenthal ET, Youngblom J, Distel D and Hunt T (1983) Cyclin: a protein specified by maternal mRNA in sea urchin eggs that is destroyed at each cleavage division. *Cell*, **33** (2) 389–96

Fang G, Yu H and Kirschner MW (1998) The checkpoint protein Mad2 and the mitotic regulator Cdc20 form a ternary complex to control anaphase initiation. *Genes Dev.* **12** 1871-1883

Forbes SA, Bhamra G, Bamford S, Dawson E, Kok C, Clements J, Menzies A, Teague JW, Futreal PA an Stratton MR (2008) The catalogue of somatic mutations in cancer. *Curr Protoc Hum Genet,* Chapter: 10; Unit 10.11

Forbes SA, Bindal N, Bamford S, Cole C, Kok C, Beane D, Jia M, Shephard R, Leung K, Menzies A, Teague JW, Campbell PJ, Stratton MR and Futreal PA (2011) COSMIC: mining the complete cancer genomes in the catalogue of somatic mutations in cancer. *Nucl Acid Res*, **39** (suppl. 1) D945-D950

Fujii T, Nomoto S, Koshikawa K, Yatabe Y, Teshigawara O, Mori T, Inoue S, Takeda S an Nakao A (2006) Overexpression of pituitary tumour transforming gene 1 in HCC is associated with angiogenesis and poor prognosis. *Hepatology*, **43** (6) 1267-1275

Funabiki H, Kumada K and Yanagida M (1996) Fission yeast Cut1 and Cut2 are essential for sister chromatid separation, concentrate along the metaphase spindle and form large complexes. *EMBO Journal*, **15** (23) 6617-6628

Funabiki H, Yamano H, Kumada K, Nagao K, Hunt T and Yanagida M (1996) Cut2 proteolysis required for sister-chromatid separation in fission yeast. *Nature*, **381** 438-441

Genkai N, Homma J, Sano M, Tanaka R and Yamanaka R (2006) Increase expression of pituitary tumour transforming gene (PTTG)-1 is correlated with poor prognosis in glioma patients. *Oncology Reports*, **15** (6) 1569-1574

Gil-Beranbé AM, Romero F, Limón-Mortés MC and Tortolero M (2006) Protein phosphatase 2A stabilises human securing, whose phosphorylated forms are degraded via the SCF ubiquitin ligase. *Molecular and Cellular biology,* **26** (11) 4017-4027

Glotzer M, Murray A and Kirschner M (1991) Cyclin is gegraded by the ubiquitin pathway. *Nature*, **349** (6305) 132-138

Gonzalez PL, Westhorpe FG and Taylor SS (2012) The spindle assembly checkpoint. *Current Biology*, **22**, R966-R980

Hagting A, Elzen N, Vodermaier HC, Waizenegger IC, Peters JM and Pines J (2002) Human securin proteolysis is controlled by the spindle checkpoint and reveals when the APC/C switches from activation by Cdc20 to Cdh1. *J Cell Biol*. **157** 1125-1137

Hanahan D and Weinberg RA (2011) Hallmarks of cancer: the next generation. *Cell*, **144** (5) 646-674

Harper JW, Burton JL, Solomon MJ (2002) The anaphase promoting complex: its not just for mitosis any more. *Genes & Development,* **16** (17) 2179-2206

Hartwell LH and Weinhart TA (1989) Checkpoints: controls that ensure the order of cell cycle events. *Science*, **246** (4930) 639-634

Heaney A, Nelson V, Fernando M and Horwitz G (2001) Transforming events in thyroid tumorogenesis and thir association with follicular lesions. *J Clin Endocrinol Metab,* **86** 5025-5032

Heaney A, Singson R, McCabe C, Nelson V, Nakashima M and Melmed S (2000) Expression of pituitary-tumour transforming gene in colorectal tumours. *Lancet*, **26** 716-719

Hilioti Z, Chung YS, Mochizuki Y, Hardy CF and Cohen-Fix O (2001) The anaphase inhibitor Pds1 binds to the APC/C associated protein Cdc20 in a destruction box dependent manner. *Curr Biol*, **11** 1347-1352

Holloway SL, Glotzer M, King RW and Murray AW (1993) Anaphase is initiated by proteolysis rather than by the inactivation of maturation-promoting factor. *Cell*, **73** (7) 1393-1402

Holt LJ, Krutchinsky AN and Morgan DO (2008) Positive feedback sharpends the anaphase switch. *Nature*, **20** (4) 792-801

Hoyt MA, Totis L & Roberts BT (1991) *S. cerevisiae* genes required for cell cycle arrest in response to loss of microtubule function. *Cell*, **66** 507-517

Hwang LH, Lau LF, Smith DL, Mistrot CA, Hardwick KG, Hwang ES, Amom A and Murray AW (1998) Budding yeast Cdc20: a target of the spindle checkpoint. *Science*, **279**, 1041-1044

Irniger S, Piatti S, Michaelis C and Nasmyth K (1995) Genes involved in sister-shromatid separation are needed for B-type cyclin proteolysis in budding yeast. *Cell*, **81** (2) 269-278

Jallepalli PV, Waizenegger IC, Bunz F, Langer S, Specicher MR, Peters JM, Kinzler KW, Vogelstein B and Lengauer C (2001) Securin is required fro chromosomal stability in human cells. *Cell*, **105** (4) 445-457

Jensen S, Segal M, Clarke DJ and Reed SI (2001) A novel role of the budding yeast separing Esp1 in anaphase spindle elongation: evidence that proper spindle association of Esp1 is regulated by Pds1. *J. Cell. Biol*, **152** (1) 27-40

Jin L, Williamson A, Banerjee S, Philipp I and Rape M (2008) Mechanism of ubiquitin chain formation by the human anaphase promoting complex. *Cell*, **133** (4) 653-665

Kakar SS and Malik MT (2006) Suppression of lung cancer with siRNA targeting PTTG. *Int J Oncol*, **29** 387-395

Kim SH, Lin DP and Matsumoto T (1998) Fission yeast Slp1: and effetor of the Mad2 dependent spindle checkpoint. *Science*, **279** 1045-1047

King RW, Peters JM, Tugendreich S, Rolfe M, Hieter P and Kirschner MW (1995) A 20S complex containing Cdc27 and Cdc16 catalyses the mitosis-specific conjugation of ubiquitin to Cyclin-B. *Cell*, **81** (2) 279-288

Kumada K, Nakmura T, Nago K, Funabiki H, Nakagawa T and Yanagida M (1998) Cut 1 is loaded onto the spindle by binding to Cut2 and promotes anaphase spindle movement upon Cut2 proteolysis. *Current Biology*, **8** (11) 633-641

Lara-Gonzalez P, Westhorpe FG and Taylor SS (2012) The spindle assembly checkpoint. *Current Biology*, **22** (22) R966-R980

Lengauer C, Kinzler KW, and Vogelstein B (1998) Genetic instability in colorectal cancers. *Nature*, **386** 623-627

Li R and Murray A (1991) Feedback control of mitosis in budding yeast. *Cell*, **66** 519-531

Littlepage LE and Ruderman JV (2002) Identification of a new APC/C recognition domain, the A box, which is required for the cdh1-dependant destruction of the kinase aurora A during mitotic exit. *Genes Dev,* **16** 2274-2285

Mailand N and Diffley JFX (2005) CDKs promote DNA replication origin licensing in human cells by protectin Cdc6 from APC/C dependent proteolysis. *Cell*, **122**, 915-926

McCabe CJ and Gittoes NJ (1999) PTTG – a new pituitary tumour transforming gene. *Journal of Endocrinology*, **162** (2) 163-166

McCabe CJ, Khaira JS, Bolaert K, Heaney AP, Tannahill LA, Hussain S, Mitchell R, Olliff J, Sheppard MC, Franklyn JA and Gittoes NJL (2003) Expression of pituitary tumour transforming gene (PTTG) and fibroblast growth factor-2 (FGF-2) in human pituitary adenomas: relationships to clinical tumour behavoir. *Clinical Endocrinology,* **58** (2) 141-150

Mora-Santos M, Castilla C, Herrero-Ruiz J, Giráldez S, Limón-Morés MC, Sáez C, Japón M, Tortolero M and Romero F (2013) A single mutation in securing induces chromosomal instability and enhances cell invasion. *European Journal of Cancer*, **49** (2) 500-510

Mussachio A & Salmon ED (2007) The spindle-assembly checkpoint in space and time. *Nature Reviews Molecular Cell Biology*, **8** (5) 379-393

Nasmyth K, Peters JM and Uhlmann F (2000) Splitting the chromosome: cutting the ties that bind sister chromatids. *Science*, **288** (5470) 1379-1384

Nurse P (1975) Genetic control of cell size at cell division in yeast. *Nature*, 547–5

Ogbagbriel S, Fernando M, Wang Z and Melmed S (2005) Securin is overexpressed in breast cancer. *Mod Pathol*, **18**, 985-990

Panguluri SK, Yeakel C and Kakar SS (2008) PTTG: and important target gene for ovarian cancer therapy. *Journal of Ovarian Research*, **1** 6

Passmore LA and Barford D (2005) Coactivator functions in a stoichiometric complex with anaphase promoting complex/cyclosome to mediate substrate recognition. *EMBO*, **6** (9) 873-878

Passmore LA, McCormack EA, Au SWN, Paul A, Willison K, Harper JW and Barford D (2003) Doc1 mediates the activity of the anaphase promoting complex by contributing to substrate recognition. *EMBO*, **22** (4) 786-796

Pei L and Melmed S (1997) Isolation and characterisation of a pituitary tumour-transforming gene (PTTG). *Molecular Endocrinology,* **11** (4) 433-

Peters JM (2006) The anaphase promoting complex/cyclosome:a machine designed to destroy. *Nat Rev Mol Cell Biol* **7** 644-656

Peterson BO, Wagener C, Marinoni F, Kramer ER, Melixetian M, Lazzerini DE, Gieffers C, Matteucci C, Peters JM and Helin K (2000) Cell cycle- and cell growth-regulated proteolysis of mammalian Cdc6 is dependent on APC-CDH1. *Genes & Development*, **14** (18) 2330-2343

Pfleger C and Kirschner M (2000) The KEN box: an APC recognition signal distinct from the D box targeted by Cdh1. *Genes & Development*, **14** (6) 655-665

Puri R, Tousson A, Chen L and Kakar S (2001) Molecular cloning of pituitary tumour transforming gene 1 from ovarian tumours and its expression in tumours. *Cancer Letters*, **163** 131-139

Reider CL, Cole RW, Khodjakov A and Sluder G (1995) The checkpoint delaying anaphase in response to chromosome monoorientation is mediated by an inhibitory signal produced by unattached kinetochores. *J Cell Biol*, **130** 941-948

Reider CL, Schultz A, Cole R and Sluder G (1994) Anaphase onset in vertebrate somatic cells is controlled by a checkpoint that monitors sister kinetochore attachment to the spindle. *J Cell Biol.* **127** 1301-1010

Reis A, Levasseur M, Chang HY, Elliott DJ and Jones KT (2006) The CRY box: a second APCcdh1 dependant degron in mammalian cdc20. *EMBO Rep,* **7** 1040-1045

Romos-Morales F, Domínguez A, Romero F, Luna R, Multon MC, Pintor-Toro JA and Tortolero M (2000) Cell cycle regulated expression and phosphorylation of *hpttg* proto-oncogene product. *Oncogene*, **19** 403-409

Shah OJ, Ghosh S and Hunter T (2003) Mitotic regulation of ribosomal S6 kinase 1 involves Ser/Thr, Pro phosphorylation of concensus and non-concensus sites by Cdc2. *Journal of Biological Chemistry*, **278** 16433-16442

Shibata Y, Haruki N, Kuwabara Y, Nishiwaki T, Kato J, Shinoda N, Sato A, Kimura M, Koyama H, Toyama T, Ishiguro H, Kudo J, Terashita Y, Konishi S and Fujii Y (2002) Expresstion of PTTG (pituitary tumour transforming gene) in esophageal cancer. *Jpn J Clin Oncol*, **32** (7) 233-237

Solbach C, Roller M, Eckerdt F, Peters S and Knecht R (2006) Pituitary tumour transforming gene expression is a prognostic marker for tumour recurrence in squamous cell carcinoma of the head and neck. *BMC Cancer,* **6** 242

Solbach C, Roller M, Fellbaum C, Nicoletti M and Kaufmann M (2004) PTTG mRNA expression in primary breast cancer: a prognostic marker for lymph node incasion and tumour reoccurance. *Breast*, **13** 80-81

Stephens PJ, Tarpey PS, Davies H, Loo PV, Greenman C, Wedges DC, Nik-Zainal S, Martin S, Varela I, Bignell GD, Yates LR, Papaemmanuil E, Beare D, Butler A, Cheverton A, Gamble J, Hinton J, Jia M, Jayakumar A, Jones D, Latimer C, Lau KW, McLaren S, McBride DJ, Menzies A, Mudie L, Raine K, Rad R, Chapman MS, Teague J, Easton D, Langerød A, OSBREAC, Lee MTM, Shen CY, Tee BTK, Huimin BW, Broeks A, Vargas AC, Turasvili G, Martens J, Fatima A, Miron P, Chin SF, Thomas G, Boyault S, Mariani O, Lakhani SR, van de Vijver M, vn 't Veer L, Foekens J, Desmedt C, Sotiriou C, Tutt A, Caldas C, Reis-Filho JS, Aparicio SAJR, Salomon AV, Børresen-Dale AL, Richardseon AL, Campbell PJ, Futrel PA and Stratton MR (2012) The landscape of cancer genes and mutational processes in breast cancer. *Nature*, **486** (7403) 400-404

Sudakin V, Chan GK and Yen TJ (2001) Checkpoint inhibition of the APC/C in HeLa cells is mediated by a complex of BUBR1, BUB3, Cdc20 and MAD2. *J Cell Biol.* **154** 925-936

Tfelt-Hansen J, Kanuparthi D and Chattopadhyay N (2006) The emerging role of the pituitary tumour transforming gene in tumorogenesis. *Clin Med Res*., **4** (2) 130-137

University of Leicester (2013) The cell cycle, mitosis and meiosis [online] Available at: http://www2.le.ac.uk/departments/genetics/vgec/highereducation/topics/cellcycle-mitosis-meiosis/ [Accessed 11.05.2013]

Yamamoto A, Guacci V and Koshland D (1996) Pds1p, an inhibitor of anaphase in budding yeast, plays a critical role in the APC and checkpoint pathway(s). *JCB*, **133** (1) 99-100

Yu R, Heaney AP, Lu W, Chen J and Melmed S (2000) Pituitary tumour transforming gene causes aneuploidy and p53-dependent and p53-independent apoptosis. *Journal of Biological Chemistry*, **275** 36502-36505

Zhang X, Horwitz GA, Prezant TR, Valentini A, Nakashima M, Bronstein MD and Melmed S (1999) Structure, expression, and function of human pituitary tumour-transforming gene (PTTG). *Molecular Endocrinology*, **13** (1) 156-166

Zou H, McGarry TJ, Bernal T and Kirschner MW (1999) Identification of a vertebrate sister-chromatid separation inhibitor involved in transformation and tumerogenesis. *Science*, **285** 418-422

Zur A and Brandeis M (2001) Securin degradation is mediated by fzy and fzr, and is required for complete chromatid separation but not for cytokinesis. *EMBO*, **20** (4) 792-801

UNIVERSITY OF BIRMINGHAM

PROJECT TWO:

The Role of Vascular Endothelial Growth Factor in Decidualisation

This project is submitted in partial fulfilment of the requirements for the award of MRes Biomedical Research

This project was carried out under the supervision of:

Dr Sarah Conner and Dr Peter Hewitt

Abstract

Vascular endothelial growth factor (VEGF) is a vital part of the decidualisation mechanism that prepares the endometrium for implantation of a blastocyst. Its integral role in the vascular reorganisation that occurs during decidualisation has long been established, however its role in decidualised stromal cells remains to be seen. It has been reported to be expressed in primary endometrial stromal and decidual cells, and more recently in an immortalised stromal cell line, St-T1b. This study hypothesises that VEGF is expressed upon decidualisation of stromal cells in response to cAMP stimulation, potentially through activation of the FOX1 transcription factor. We aimed to successfully decidualise St-T1b cells through progesterone and cAMP stimulation, examine VEGF expression at short decidual time points, and investigate potential VEGF gene regulation. Results suggest that VEGF expression increases upon decidualisation in a manner related to FOXO1 expression, and that VEGF expression by decidual cells has potential function implications.

Acknowledgements

I would like to thank Dr Sarah Conner and Dr Peter Hewitt for all their encouragement, guidance and patience throughout my time in the lab. Thanks also to the rest of the lab for their help and support.

Table of Contents

1.0 INTRODUCTION **7**

1.1 MENSTRUAL CYCLE 7

1.2 FERTILISATION AND EARLY EMBRYO DEVELOPMENT 10

1.3 DECIDUALISATION 13

1.5 VEGF AND DECIDUALISATION 17

1.7 AIMS AND OBJECTIVES 19

2.0 MATERIALS AND METHODS **20**

2.1.1 Cell Lines *20*

2.1.2 Maintenance of Cell Lines *21*

2.2 PLASMIDS AND TRANSFECTIONS 21

2.2.1 Plasmids *21*

2.2.2 Transient Transfection *22*

2.3 DECIDUALISATION AND ANALYSIS OF ST-T1B CELLS 23

2.3.1 Stimulation of Cells *23*

2.3.3 cDNA synthesis *24*

2.3.4 PCR *27*

2.3.5 VEGF ELISA *27*

2.5 SPHEROIDS 27

2.5.1 Spheroid Production *27*

2.5.2 Sprouting Assays *28*

2.6 FOXO1 AND VEGF IMMUNOFLUORESCENCE 29

2.6.1 Cell Culture on Microculture Slides *29*

2.5 STATISTICAL ANALYSIS 30

3.0 RESULTS **32**

3.1 DECIDUALISATION OF ST-T1B CELLS 32

3.2 VEGF IS UP-REGULATED IN ENDOMETRIAL STROMAL CELLS FOLLOWING DECIDUALISATION 35

3.3 LOCALISATION OF VEGF AND FOXO1 IN DECIDUALISING ST-T1B CELLS. 35

3.5 INCUBATION OF ST-T1B CELLS WITH DECIDUALISATION MEDIUM DECREASES VEGF PROMOTER ACTIVITY. 41

3.6 HTR8 SPROUTING DECREASES WITH VEGF STIMULATION 44

3.7 HTR8 SPROUTING DECREASES WHEN INCUBATED WITH E2 AND CONDITIONED DECIDUALISATION MEDIUM 47

4.0 DISCUSSION 51

5.0 REFERENCES 57

List of Figures and Tables

Figure 1: The Menstrual Cycle **75**

Figure 2: Early Embryo Development **78**

Figure 3: FOXO1 Regulation in Decidual Cells **82**

Table 1: List of PCR Primers **91**

Table 2: List of PCR Conditions **92**

Table 3: Statistical Significance Key **97**

Figure 4: Morphological Change and FOXO1 Localisation in Decidualised St-T1b Cells **99**

Figure 5: Detection of dProlactin in Deciudualised St-T1b Cells by PCR **100**

Figure 6: Up-regulation of VEGF in St-T1b Following Decidualisation **102**

Figure 7: Up-regulation of VEGF in Decidualised St-T1b Cells Over Time **103**

Figure 8: Localisation of VEGF and FOXO1 in St-T1b Cells **105**

Figure 9: FOXO1 Increases VEGF Promoter Activity **108**

Figure 10: VEGF Promoter Activity in St-T1b Cells **109**

Figure 11: HTR8 Spheroid Sprouting is reduced with VEGF **111**

Figure 12: HTR8 Spheroid Sprouting is inhibited by VEGF **112**

Figure 13: HTR8 Spheroid Sprouting is reduced with Decidualised St-T1b Conditioned Medium **114**

Figure 14: Decidualised St-T1b Conditioned Medium inhibits HTR8 Spheroid Sprouting **115**

1.0 Introduction

It's been 35 years since the first successful pregnancy from IVF (*in vitro* fertilisation) (Steptoe & Edwards, 1978). Since that time Assisted Reproduction Techniques, or ART, have advanced dramatically, yet there still remain discrepancies between IVF fertilisation rate and live birth rate following transfer of IVF embryos. A study by Malizia et al. (2009) examined data from 6000 IVF patients and established that the live birth success rate after three cycles of IVF treatment stood at 45% and at 51% following six cycles of treatment.

Success is influenced by many factors including maternal age, and embryo quality. Embryo screening protocols select the best –embryos, and therefore those most likely to progress to full term, are transferred (Puissant et al., 1987). Despite these measures being in place there remains a high rate of unsuccessful pregnancies, suggesting that other factors affecting the implantation process may contribute to infertility levels in these patients. It is therefore paramount to investigate the environment in which the transferred embryo must survive, in order to understand why the live birth rate following IVF treatment remains low.

1.1 Menstrual Cycle

The menstrual cycle is comprised of two phases; the follicular phase, which precedes ovulation, and the luteal phase, which precedes menstruation. The cycle is controlled by several factors including; the female sex hormones Oestrogen and

progesterone, which predominantly control the cycle; follicle stimulating hormone (FSH) and luteinising hormone (LH) which are involved in ovulation; and inhibins A and B which are involved in regulation of FSH and LH (Johnson & Everitt, 2007). At low levels Oestrogen negatively regulates FSH and LH preventing follicle stimulation, and at high levels it positively regulates FSH and LH leading to follicular maturation and selection (Johnson & Everitt, 2007). Progesterone regulates oestrogen, causing it to fall and hence preventing negative regulation of FSH and LH by oestrogen (Johnson & Everitt, 2007).

The cycle begins with loss of the endometrium in response to falling oestrogen and progesterone levels (Figure 1) (Straussman, 1998; Jabbour et al., 2006). Stromal cells of the endometrium detect the decline in progesterone, triggering an enzyme cascade that results in influx of leukocytes, constriction of spiral blood vessels, expression of VEGF, and shedding of the endometrium (menstruation) (Straussman, 1998).

The follicular phase follows menstruation. Follicles in the ovary are stimulated to grow by oestrogen. The endometrial cells begin to proliferate and the lining of the womb begins to grow (Mihm, Gangooly & Muttukirshna, 2010). The most dominant follicle induces an increase in oestrogen and inhibin A, which in turn lead to a dramatic rise in FSH and LH levels causing ovulation to occur (Figure 1). Upon ovulation oestrogen levels begin to decline, followed by an equally dramatic decrease in LH and FSH (Figure 1). At this point progesterone levels begin to increase and the follicular phase ends.

Figure 1: The Menstrual Cycle

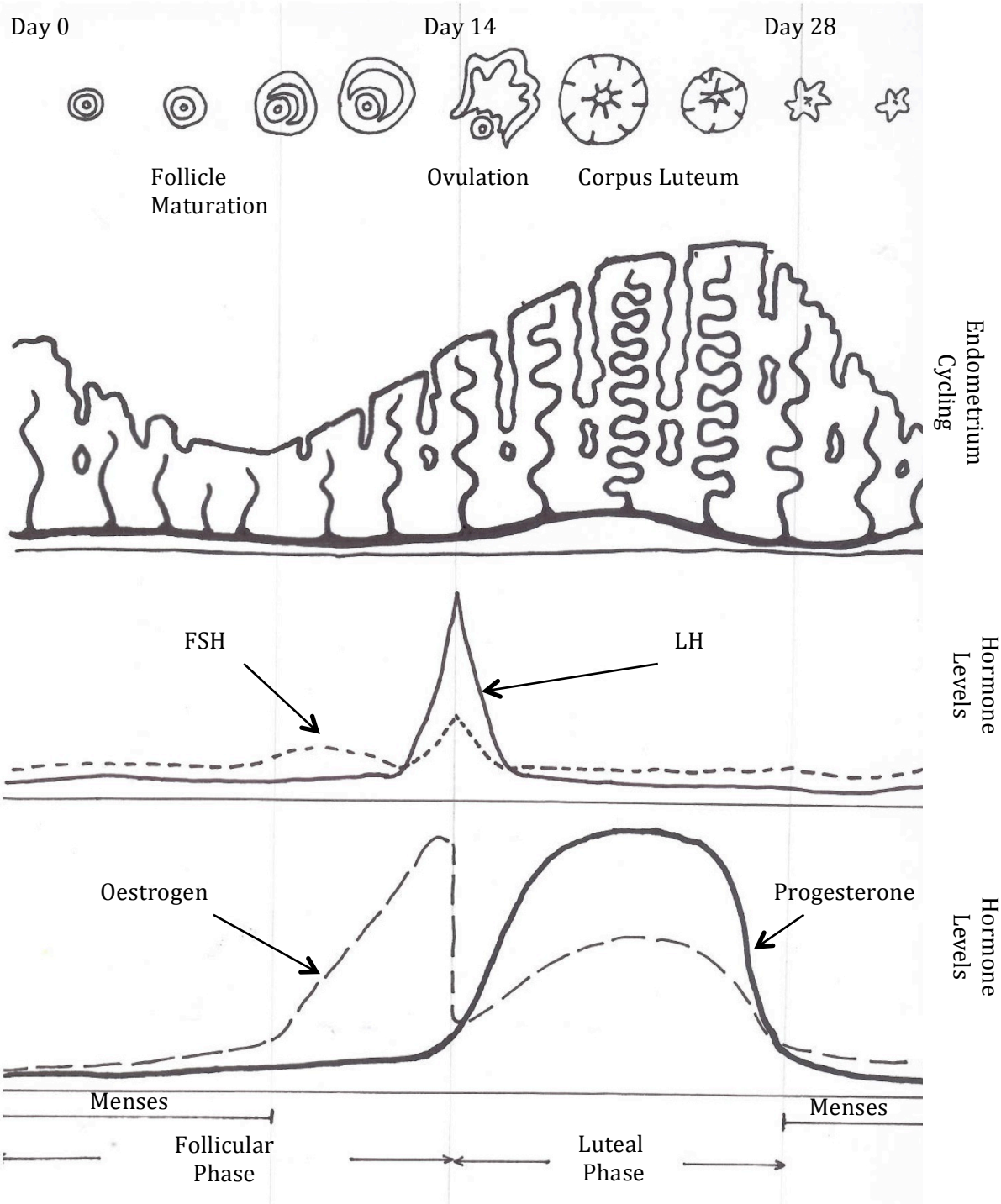

Figure 1: The menstrual cycle. The various changes that occur in the menstrual cycle, highlighting follicular development, ovulation, and corpus luteum formation, corpus luteum degradation; endometrial cycling and hormonal changes in the 28 day cycle. (Where FSH = follicule stimulating hormone, and LH = lutenising hormone).

The luteal phase begins with the formation of the corpus luteum from the ruptured dominant follicle left behind following ovulation, a rise in progesterone levels, and differentiation of the endometrium (Figure 1) (Mihm, Gangooly & Muttukirshna, 2010). The corpus luteum expresses both inhibin A and oestrogen, however the high levels of progesterone inhibits the negative feedback effects of oestrogen on FSH and LH, ensuring that their levels remain low, and preventing further follicle stimulation (Figure 1). If fertilisation of the ovulated egg does not occur then the corpus luteum breaks down, both progesterone and oestrogen levels decline, and the luteal phase ends (Figure 1) (Straussman, 1998). This leads to the endometrium being shed and the cycle begins again (Figure 1). If fertilisation does occur progesterone persists at high levels, and the corpus luteum remains intact to prevent further follicular development, and loss of the endometrium (Straussman, 1998).

1.2 Fertilisation and Early Embryo Development

After ovulation occurs the oocyte is transported down the fallopian tube by cilia and peristaltic movements (Noorwood et al., 1978) (Figure 2). Spermatozoa have to overcome many barriers in their journey to the ovulated oocyte, with fewer than 1 in 1,000,000 reaching the site of the oocyte (Johnson & Everitt, 2007). Sperm undergo several changes that affect their morphology and metabolism in order to be capable of fertilisation (Johnson & Everitt, 2007). These changes include; maturation in the male tract, particularly in the epididymis; hyper mobility through a process called capacitation; and the acrosome reaction which occurs within the female tract (Hinrichsen & Blaquier, 1980; Salicioni et al., 2007; Osman et al., 1989).

Capacitation causes the spermatozoa to gain hyper mobility, and also enables them to detect the oocyte through olfactory sensors by chemotaxis (Johnson & Everitt, 2007; Olsson & Laska 2010) (Figure 2). Upon locating the oocyte the spermatozoa bind to the zona pellucida which surrounds the ovulated oocyte. Here the spermatozoa undergo the acrosome reaction, prompted by signalling from the oocyte, which allows the sperm to digest a section of the ZP and enter the perivitelline space (Osman et al., 1989). Here a spermatozoon is able to come into direct contact with the membrane of the oocyte. It binds, and fuses to the oocyte membrane and the nuclear content enters the oocyte's cytoplasm (Reviewed by Kaji & Kudo, 2004). Simplistically, upon entry to the oocyte's cyctoplasm the nuclear membrane breaks down, pro-nuclei form around both the male and female sets of chromosomes, and they gravitate towards one another to the centre of the oocyte (Johnson & Everitt, 2007). DNA synthesis occurs before the pronuclei breaks down, chromosomes align upon the metaphase plate and the first mitotic division occurs 24 hours after fertilisation, and the fertilised oocyte is now known as the conceptus (Johnson & Everitt, 2007) (Figure 2).

Throughout the early stages of development, the conceptus remains the same size, however the cell (blastomere) number within the conceptus increases with every division (Johnson & Everitt, 2007) (Figure 2). By the 8 cell conceptus a sequence of events leading to morphology changes begin. The morula forms, and just after the conceptus enters the uterus, around 4.5 days, it develops into a blastocyst (Johnson &

Figure 2: Early Embryo Development

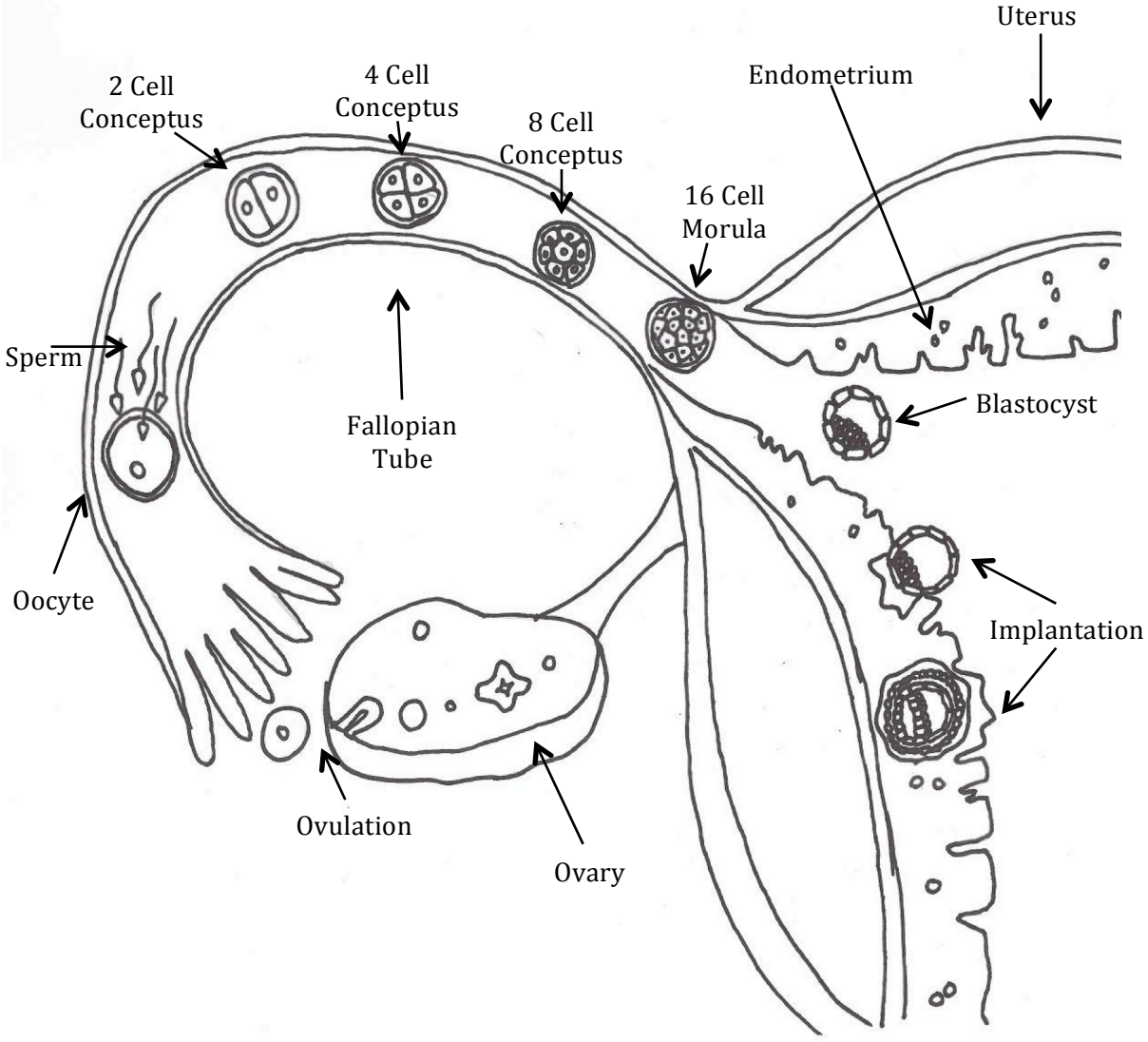

Figure 2: Early embryo development. Diagram of the female reproductive organs, demonstrating the journey of the ovulated oocyte, fertilisation, and development of the conceptus prior to implantation.

Everitt, 2007) (Figure 2). Blastocyst development initiates differentiation of the blastomeres into either trophoblasts, which create a barrier to the uterine environment, or pluriblasts, which become the inner cell mass (Johnson & Everitt, 2007). At this point the blastocyst sheds the zona pellucida and prepares for implantation into the endometrium (Figure 2).

1.3 Decidualisation

In order for implantation of the blastocyst to occur, changes to the endometrium must occur simultaneously to early embryo development. This creates a 'window of receptivity' when implantation can occur, where both the conceptus and the endometrium must have reached the correct stage of development at the same time (Psychoyos, 1976). This change to the endometrium is called decidualisation, where along with increased vascularisation, and an increase in immune cells, stromal cells differentiate into decidual cells in response to hormonal changes in the menstrual cycle (Johnson & Everitt, 2007). The process is vital to both the normal menstrual cycle and pregnancy, and occurs independently of the presence of a blastocyst (Mihm, Gangooly & Muttukrishna, 2010).

Upon decidualisation, endometrial stromal cells undergo morphological changes becoming less elongated and more rounded, metabolic changes occur, and the proteins expressed by the cells change (Oliver 1999; Brar 2001). In particular decidualised prolactin (dProlactin) and insulin-like growth factor binding protein 1 (IGFBP1) are

markers of decidualisation (Daly et al., 1983; Tseng et al., 1992; Telgmann & Gellerson, 1998).

The stromal to decidual cell transition requires both progesterone, and cyclic adenosine monophosphate (cAMP) (Brosens et al., 1999; Tankana et al., 1993; Telgmann & Gellerson 1998). Levels of cAMP are regulated by hormones such as pituitary gonadotrophins, prostaglandin E_2 and relaxin (Tankana 1993; Gellerson & Brosens 2003). These hormonal signals initiate an enzyme cascade through G-coupled protein receptors (GPCR) (Telgmann et al., 1997) which activate andenylyl cyclase, producing cAMP (Telgmann et al., 1997). The cAMP activates downstream protein kinase A (PKA) signalling leading to activation of transcription factors involved in promoting the expression of decidual specific genes (Telgmann et al., 1997). If the cAMP stimulus is removed decidual cells revert back to stromal cells, the PKA pathway has to be maintained continuously in order for the decidual cells to remain differentiated (Telgmann et al., 1997).

Prolactin is a specific marker for decidualisation (Daly et al., 1983; Telgmann & Gellerson, 1998). The action of cAMP upon decidualising cells initiates prolactin expression in a number of ways. Firstly, cAMP via the PKA pathway, induces expression of CCAAT/enhancer binding protein β (C/EBPβ) a leucine zipper transcription factor (Landschulz, Johnson & McKnight, 1998; Pohnke, Kempf & Gellerson, 1999). C/EBPβ binds to a decidual-specific promoter region of prolactin and promotes its expression (Pohnke, Kempf & Gellerson, 1999). Secondly, cAMP also induces expression of FOXO1 a member of the FKHR (forkhead homologue in

rhabdomyosarcoma) transcription factor family (Davies et al., 1995). FOXO1 and C/EBPβ work in a synergistic manner at the decidual-specific prolactin promotor site to stimulate prolactin expression (Christian et al., 2002).

FOXO1 is involved in regulation of many integral cell functions including metabolism, and apoptosis (Reviewed by Katoh, 2004). Its intimate involvement in the apoptosis pathway means that it needs to be closely regulated so to promote survival. FOXO1 expression is induced upon differentiation of stromal cells to decidual cells (Labied et al., 2006). Its activity depends upon its localisation within the cell, which is highly regulated by the phosphoinositol-3 kinase (PI3K) pathway (Tang et al., 1999; Labied et al., 2006) (Figure 3). Normally, the PI3K pathway is stimulated leading to phosphorylation of the serine/threonine kinase Akt (Tang et al., 1999). Activated Akt, phosphorylates FOXO1, leading to exclusion from the nucleus and localisation in the cytoplasm preventing its function as a transcription factor (Tang et al., 1999). In decidual cells this process is inhibited by cAMP, which promotes nuclear localisation of FOXO1, however progesterone promotes the PI3K signalling pathway causing FOXO1 to be localised to the cytoplasm (Christian et al., 2002; Labied et al., 2006) (Figure 3). This concept becomes easier to understand in the context of the menstrual cycle. During the luteal phase when progesterone levels are high the cytoplasmic localisation of FOXO1 promoted through the PI3K pathway is maintained (Labied et al., 2006) (Figure 3). However, at the onset of menstruation, progesterone levels decrease and FOXO1 remains localised at the nucleus through cAMP signalling initiating apoptotic pathways and endometrial breakdown (Brosens & Gellerson, 2006) (Figure 3). This is a prime

Figure 3: FOXO1 Regulation in Decidual Cells

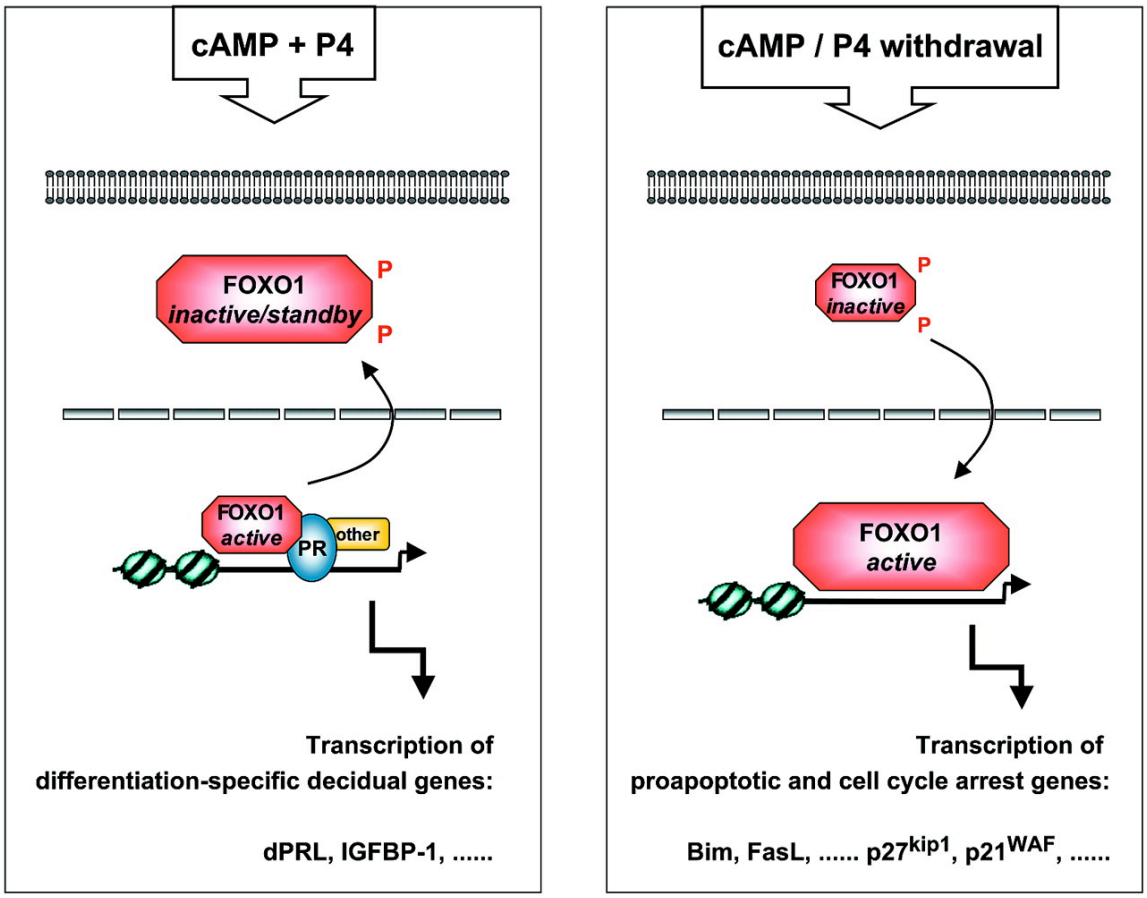

Figure 3: FOXO1 regulation in decidual cells. Regulation of FOXO1 by phosphorylation in response to stimulation by cAMP and progesterone (P4). (Source: Brosens & Gellerson, 2006).

example of the delicate balance of regulation that must occur within decidual cells to promote survival (Brosens & Gellersen, 2006).

Along with distinct changes at the cellular level, decidualisation also requires changes to the endometrial tissue organisation (Reviewed by Plasier, 2011). Amongst other changes, the endometrium undergoes extensive re-modelling of its vascular system in anticipation for implantation. This remodelling involves a number of angiogenic proteins including vascular endothelial growth factor A (from this point onwards VEGF).

1.5 VEGF and Decidualisation

VEGF is an integral part of the mechanisms underlying the major reorganisation of vasculature during decidualisation of the endometrium (Plasier, 2011). VEGF is strongly up-regulated by hypoxia in the endometrium to induce angiogenesis, and therefore is critical for implantation, and maintenance of the maternal-foetal blood supply (Sharkey et al., 2000; Plasier et al., 2011). It is thought that immune cells including machrophages, neutrophils uterine natural killer cells are a major source of VEGF in endometrial tissue (Charnock-Jones et al., 2000; Mueller et al., 2000; Li et al., 2001; Jabbour et al., 2006).

The expression and function of VEGF in endometrial stromal and decidual cells is not fully understood. Studies using primary human endometrial stromal cells have shown that VEGF is expressed in response to both oestrogen and progesterone (Sugino

et al., 2002). Primary decidual cells also express VEGF in response to both hypoxia and stimulation by cAMP suggesting that pathways downstream of cAMP may also regulate VEGF expression (Popovici et al., 1999). The relationship between VEGF expression and decidualisation is an important one, as VEGF has been found to promote not only angiogenesis, but also cell survival (Spyridopoulos et al., 1996; Gerber et al., 1998; Gerber et al., 1998). For example in endothelial cells, VEGF inhibits TNF-α induced apoptosis, and also has been found to promote cell survival through the PI3K/Akt pathway (Spyridopoulos et al., 1996; Gerber et al., 1998). Additionally, in human umbilical vein endothelial cells VEGF induces expression of the antiapoptotic factors, Bcl-2 and A1 (Gerber et al., 1998). Primary decidual cells have been found to express the two VEGF receptors Flt1 and KDR, therefore it is possible that VEGF stimulates cell survival in decidualised endometrial stromal cells through similar mechanisms (Sugino et al., 2002). VEGF expression by decidual cells may also have an effect on the implanting trophoblast cells, particularly as they too express the VEGF receptors Flt1 (fms-related tyrosine kinase 1) and KDR (kinase insert domain receptor) (Shore et al., 1997).

The recently characterised St-T1b stromal cell line produced through retroviral-mediated human telomerase over-expression, can be differentiated by stimulation with progesterone and cAMP, and therefore provide an experimental model, alternative to primary endothelial stromal cells (Samalecos et al., 2009). A proteasome profile for St-T1b cells has identified that VEGF is highly expressed in decidualised cells, and therefore is the ideal model for investigating VEGF expression in decidual cells (Schwenke et al., 2013).

1.7 Aims and Objectives

Considering the plethora of literature concerning the function of VEGF in vascular remodelling in decidualisation, very little is known about the regulation and role of VEGF in endometrial stromal and decidual cells (Charnock-Jones et al., 2000; Plasier et al., 2011). Owing to its ability to function as an angiogenic factor in the endometrium, and its ability to stimulate cell survival mechanisms in endothelial cells, VEGF may elicit similar effects in differentiated stromal cells (Sugino et al., 2002). In addition to inflammatory cells the decidualised stromal cells may represent a significant source of VEGF.

We hypothesise that VEGF is up-regulated in endometrial stromal cells in response to cAMP stimulated pathways through FOXO1 activation. In this project the human St-T1b cell line was used as a stromal cell model to:

- Establish and characterise decidualisation through treatment with progesterone and cAMP.
- To investigate the pattern of VEGF expression following stimulation of cells with progesterone and cAMP stimulation andassess the potential involvement of FOXO1 in this process.
- To determine whether conditioned medium from decidualised stromal cells influences the invasive properties of trophoblasts.

2.0 Materials and Methods

2.1 Cell Lines and Culture Conditions

2.1.1 Cell Lines

The HEK-293 human embryonic kidney cells, were obtained from the ATCC, and cultured in Dulbecco's Modified Eagle's Medium (DMEM), containing 10% foetal bovine serum (FBS), L-Glutamine and 50 I.U./ml Penicillin and 50 (µg/ml) Streptomycin (Pen/Strep) (Graham et al., 1977). HEC1-B cells are a human endometrial carcinoma cell line and were cultured in DMEM/Ham F-12, 10% FBS, L-Glutamine and Pen/Strep (Kuramoto, 1972). The HTR-8/SVneo (HTR-8) human trophoblast cell line was derived from first trimester trophoblasts immortalized using the SV40 large T antigen and kindly provided by Dr. Charles Graham (Department of Anatomy & Cell Biology, Queen's University at Kingston, Ontario, Canada)(Graham et al., 1993). HTR-8 cells were cultured in Roswell Park Memorial Institute (RPMI)-1640 medium, containing 10% FBS, L-Glutamine, and Pen/Strep. The St-T1b human endometrial stromal cell line were established through retroviral-mediated human telomerase over-expression (Samalecos et al., 2009) and kindly provided by Dr. Birgit Gellersen (Endokrinologikum, Hamburg, Germany). St-T1b cells were cultured in growth medium comprising DMEM/F-12, 10% FBS, I nM Oestradiol, 1 µg/ml Insulin, L-Glutamine, and Pen/Strep.

2.1.2 Maintenance of Cell Lines

Typically cells were grown in T75, or T25 flasks and passaged once confluent. Culture medium was aspirated and cells were washed gently with PBS (phosphate-buffered saline) before adding 1ml Trypsin and incubating at 37^{O}C for 5 minutes. After incubation with trypsin, 8 ml of culture medium was added, and cell density was calculated using a haemocytometer. Cells were then plated at the desired density.

2.2 Plasmids and Transfections

2.2.1 Plasmids

Fragments (1.8, 2.9 and 4.7 Kb) of the human VEGF-A promoter, cloned into the pGL-2 luciferase reporter vector (Promega), were kindly provided by Dr Sheela Jayaraman (School of Immunity and Infection, University of Birmingham). The plasmids were transformed into *E. coli* (Bioline) and grown overnight on LB agar. Colonies were picked and grown overnight in 10 ml LB Broth, with agitation at 37^{O}C. The cultures were scaled up to 100 ml LB Broth, and again grown up overnight with agitation at 37^{O}C. The plasmids were extracted using an Endotoxin-free Maxi DNA kit (QIAgen) and concentration determined using a spectrophotometer.

2.2.2 Transient Transfection

Transfections were carried out in HEK-293 and St-T1b cells primarily using ExGen500 (Fermentas), however transfection efficiency was tested using Fugene 6 (Promega), Lipofectamine 2000 (Invitrogen), and JetPrime (Polyplus Transfection). HEK293 cells were plated at a density of $2x10^5$ cells / well, and St-T1b cells at $1.2\ x10^5$ cells /well onto 12-well plates and incubated overnight. Prior to transfection the growth medium was aspirated from the wells and replaced with 1 ml of fresh medium. For the St-T1b cells the growth medium was supplemented with 10 ng/ml FGF for St-T1b cells. Transfections were performed with 1 μg DNA following manufacturer's guidelines and the DNA complexes added drop-wise to each well. Plates were then incubated for 48-72 hours at 37^OC. The medium in St-T1b cell transfections was aspirated after 24 hours of transfection and replaced with the appropriate medium, for the remainder of the incubation period.

2.2.3 Luciferase Reporter Assays

A Dual-Luciferase Reporter Assay (Promega) was used to determine VEGF promoter activity in transfected cells following manufacturer's guidelines, and results were normalised to Renilla luciferase reading from the co-transfected pRL-CMV control plasmid. GFP expression levels were monitored through fluorescence microscopy.

2.3 Decidualisation and Analysis of St-T1b Cells

2.3.1 Stimulation of Cells

Decidualisation of St-T1b cells was induced as described by Samalecos et al. (2009). St-T1b cells were plated onto 6-well plates and allowed to grow to confluence. The growth medium was aspirated and cells were washed once with PBS. The cells were treated with 1 ml of decidualisation medium (DMEM/F-12, 2% charcoal-stripped FBS, 1 µM MPA, 0.5 mM 8-Br-cAMP, Pen/Strep) . Control cells were incubated in 1 ml per well of oestrogen containing medium (E2 medium) (DMEM/F-12, 10% charcoal-stripped FBS, 1 nM 17-Beta-Estradiol, 1 µg/ml Insulin, Pen/Strep). Conditioned medium was collected from cells after various time periods and stored at -20^{O}C.

2.3.2 RNA Extraction

Total RNA was extracted using an RNA Extraction Kit (Norgen). Cells growing on 6-well dishes were washed with 1 ml PBS and then incubated with 175 µl/well of RNA Lysis Buffer (Total RNA extraction kit, Norgen) for 5 minutes at room temperature. The lysate from the two wells was combined and the samples stored at -20^{O}C.

Frozen samples were thawed on ice, and 600 µl of the lysate was loaded at a time onto a column and centrifuged (13,000 rpm, 1 minute) until all lysate had been

loaded onto the column. Flow through was discarded and the column was washed three times using 400 µl of the wash solution provided. Following the third wash the column was centrifuged once more at 13,000 rpm for 2 minutes to remove any excess wash solution from the column. The collection tube was discarded and replaced with a fresh RNase free Eppendorf, 50 µl of elution solution was loaded onto the centre of the column. The RNA was then eluted by one spin at 200 g for 2 minutes, followed by another spin at 14000 g for 1 minute. RNA concentration was measured on a spectrophotometer and then either used immediately to synthesise cDNA or stored at -80^{O}C.

2.3.3 cDNA synthesis

A stock solution of cDNA reaction mix (for one reaction; 1 µl Oligo $(dT)_{18}$ Primer, 1 µl 10 mM dNTP, 4 µl 5x RT buffer, 1 µl Ribosafe RNase inhibitor, 1 µl Reverse Transcriptase) was prepared using the cDNA synthesis kit (BioLine). RNA concentrations were normalised so that all cDNA reactions contained the same concentration of RNA and made up in PCR grade dH_2O to have a total volume of 12 µl. To each RNA sample 8 µl of stock solution was added. The samples were then incubated at 45^{O}C for 30 minutes, followed by 55^{O}C for another 30 minutes. Samples were either used immediately for PCR or stored at -20^{O}C.

Table 1: Table of Primers

Primers	Oligonucleotide Sequence (5'-3')	PCR Amplicon Size (bp)
dProlactin – F	GAGACACCAAGAAGAATCGGAACATACAGG-	416
dProlactin – R	TCGGGGGTGGCAAGGGAAGAA	
IGFBP1 – F	TGCTGCAGAGGCAGGGAGCCC	378
IGFBP1 - R	AAGGATCCTCTTCCCATTCCA	
GAPDH – F	CAATGACCCCTTCATTGACC	159
GAPDH - R	TTGATTTTGGAGGGATCTCG	

Table 1: A table of all PCR primers used for decidualisation analysis and their sequences

Table 2: Table of PCR Conditions

PCR Primer	PCR Conditions
dProlactin	44 Cycles: 94 ^{O}C 45 sec, 57 ^{O}C 45 sec, 72 ^{O}C 45 sec
IGFBP1	40 Cycles: 95 ^{O}C 30 sec, 63 ^{O}C 30 sec, 72 ^{O}C 60 sec
GAPDH	35 Cycles: 95 ^{O}C 30 sec, 51 ^{O}C 30 sec, 72 ^{O}C 45 sec

Table 2: PCR conditions and cycles used during amplification of cDNA products

2.3.4 PCR

Decidualisation of St-T1b cells was confirmed by RT-PCR detection of decidualised Prolactin (dProlactin) and IGFBP1 with GAPDH as a control (Samalecos et al., 2009; Frettsome, 2011). PCR primers for dProlactin, IGFBP1 and GAPDH are shown in table 1. Samples were prepared for PCR using 10 ul PCR reaction mix (BioLine), 1 ul cDNA, 0.5 ul of forward and reverse primers, and 8.5 ul of PCR grade H_2O. The PCR reactions conditions are shown in table 2.

2.3.5 VEGF ELISA

Conditioned medium collected from stimulated St-T1b cells were analysed for VEGF levels using the Human VEGF DuoSet ELISA kit (R&D Systems) following the manufacturer's guidelines.

2.5 Spheroids

2.5.1 Spheroid Production

HTR8 spheroids were produced using the method of Korff & Augustin (1998). Methylcellulose (6 g) was autoclaved, and dissolved in 250 ml RPMI-1640 preheated to $60^{O}C$ for 20 minutes. A further 250 ml RPMI 1640 was added and the solution mixed overnight at $4^{O}C$. The methylcellulose solution was centrifuged (5000g, 2 hours, room temperature) and the supernatant aliquoted for use in spheroid production.HTR8 cells

were trypsinised, and the number of cells required (750 cells per well) added to a 20% methylcellulose, 80% RPMI-1640 growth medium. Of this stock solution 150 μl was added per well of a 96 well round bottomed suspension plate (Sarstedt) and incubated for 24 hours at 37^{O}C for the spheroids to form.

2.5.2 Sprouting Assays

Sprouting assays were carried out in 24 well plates using 10-12 spheroids per well/condition. Spheroids were harvested using 200 μl pipette tips in an IVF tissue culture hood, and placed into 1 ml high serum medium (DMEM/F-12, 10% FCS, L-Glutamine, Pen / Strep) in a 6 well plate. They were then washed in another 1 ml of high serum medium by transfer into another well of the 6 well plate. Fibrinogen (3 mg/ml in DMEM/F-12) was prepared and 500 μl/well added to a 24 well plate. Spheroids (10-12/well) were transferred into the fibrinogen solution and 15 μl of thrombin was added and the plate was 'swirled' continuously to keep the spheroids suspension until the gel had set.

To each well 500 μl of the appropriate medium was added, containing 10% protenin bovine blood trypsin inhibitor to prevent degradation of the fibrinogen. The spheroids were then incubated at 37^{O}C and photographed at 24, 48, or 72 hours to monitor sprouting.

2.6 FOXO1 and VEGF Immunofluorescence

2.6.1 Cell Culture on Microculture Slides

Cells ($2x10^4$/well) were plated onto 8-well microculture slides (BD Falcon) in 300 μl of normal growth medium and incubated at 37^OC overnight. One well of HEC1B cells was plated, along with seven wells of St-T1b cells. St-T1b cells were stimulated with decidualisation medium as described above (Section 3.3.1) at various times to coincide so that all wells on the slide were fixed at the same time.

2.6.2 Fixing and Staining of Slides

Cell fixation and staining was performed at room temperature Cells were fixed for 20 minutes in fixing solution (10 mM PBS (pH 7.4), 0.9% Formaldehyde, 0.8 g Glucose) washed once in PBS, incubated for 6 minutes in 100% Methanol, and then washed twice with PBS. Samples were blocked for 20 minutes in 5% normal goat serum in PBS, followed by incubation with the primary antibodies (Polyclonal Rabbit anti-FKHR 1:50 (Santa-Cruz Biotechnology), monoclonal Mouse anti-humanVEGF 1:200 (R&D Systems) in 1% BSA in PBS). One control well was incubated without the primary antibodies.

Cells were washed twice with PBS and then incubated, with the AlexaFluor (Invitrogen) secondary antibodies (Alexafluor 594 (red) Alexafluor 430 (green) 1.5% Goat Serum in PBS) for 1 hour in the dark. The culture chamber was removed and slides were mounted using DAPI (4',6-diamidino-2-phenylindole) mounting medium.

Slides were visualised using fluorescence microscopy and photographed at x40 magnification.

2.5 Statistical Analysis

Statistical analysis was carried out using MicrosoftExcel. Where n number was less than 3 standard deviation about the mean was displayed on graphs, where n number was more than 3 standard error about the mean was used to show varience. Significance was analysed using a two-tailed, paired, student's t-test and significance was displayed as shown in table 3.

Table 3: Statistical Significance Key

P value	Key
P<0.05	*
P<0.01	**
P<0.001	***
P<0.0001	****

Table 3: Statistical significance key

3.0 Results

3.1 Decidualisation of St-T1b Cells

St-T1b cells were treated with either E2 medium or decidualising medium and harvested between 30 minutes and 72 hours, depending on the experiment. Initially there were difficulties with the St-T1b cells, they were not proliferating well or undergoing decidualisation. However, after a serum in the growth medium was changed and insulin was added to the condition of the cells vastly improved. In order to determine whether the cells were undergoing decidualisation the expression of three specific markers were examined (Daly, Maslar & Riddick, 1983; Christian et al., 2002; Salmelecos et al., 2009. Firstly, cell morphology was analysed by bright-field microscopy; secondly, FOXO1 expression and distribution was determined through fluorescent staining; and finally, dProlactin levels were determined by PCR.

Figure 4 shows the characteristic change in morphology from an elongated, fibroblast-like appearance to a more rounded epithelial cell shape as the St-T1b cells decidualised. Cytofluorescent studies revealed the up-regulation and nuclear localisation of FOXO1 after 24 hours incubation in decidualisation medium compared with control cells non-decidualised medium, and PCR showed increased dProlactin expression in St-T1b cells (Figures 4 and 5 respectively). Having determined that the St-T1b cells were readily responding to decidualisation medium at the 24 hour time point they were further analysed for FOXO1 expression over time by fluorescent staining.

Figure 4: Morphological Change and FOXO1 Localisation in Decidualised St-T1b Cells

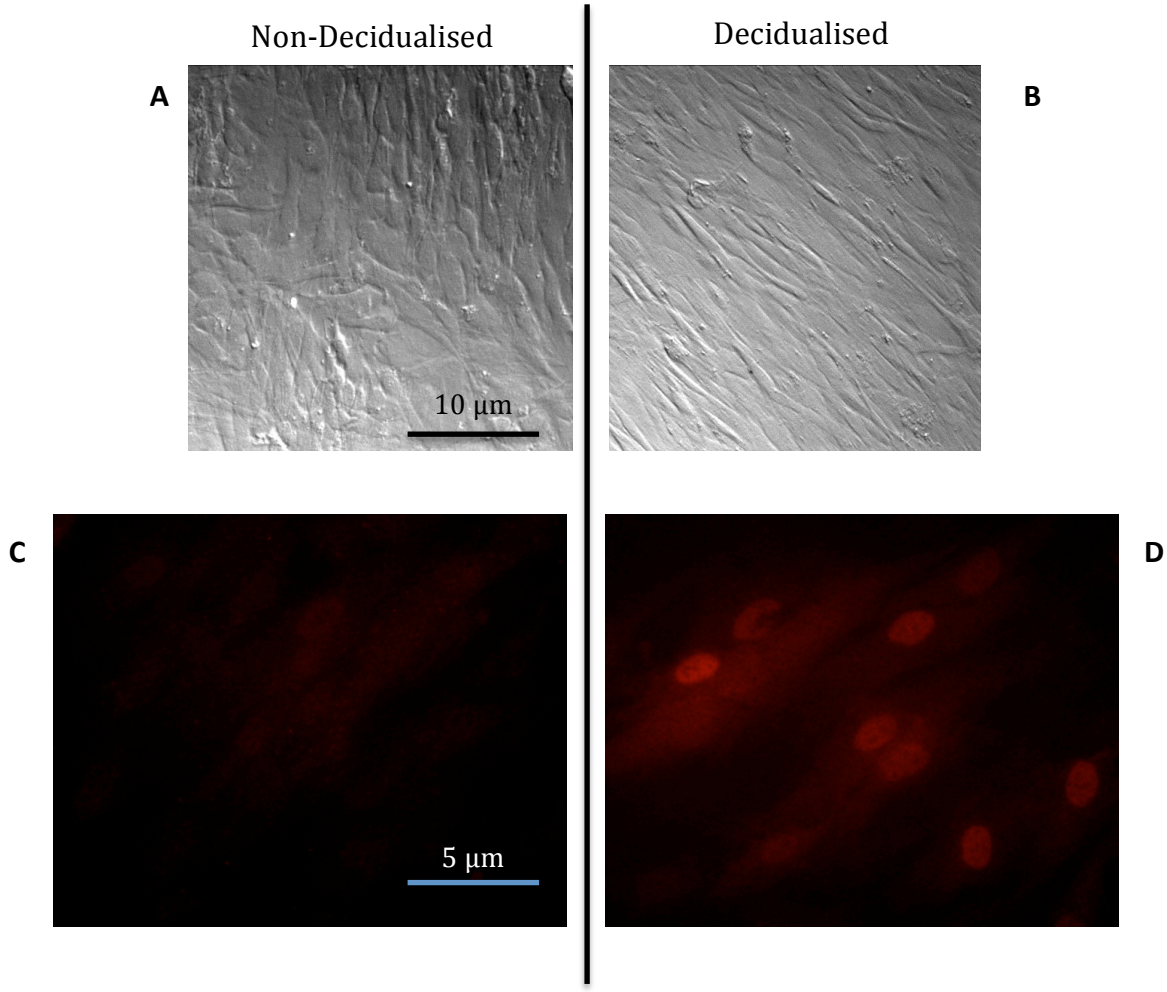

Figure 4: Morphological change and FOXO1 localisation in decidualised St-T1b cells. Representative brightfield images (x 40 objective) showing characteristic St-T1b cell morphology following 3-day incubation in (A) E2 medium and (B) decidualisation medium. FOXO1 cytofluorescent staining of St-T1b cells incubated in (C) E2 medium and (D) decidualisation medium. FOXO1 staining in (A) control and (B) decidualised St-T1b cells x 40 power.

Figure 5: Detection of dProlactin in Decidualised St-T1b Cells by PCR

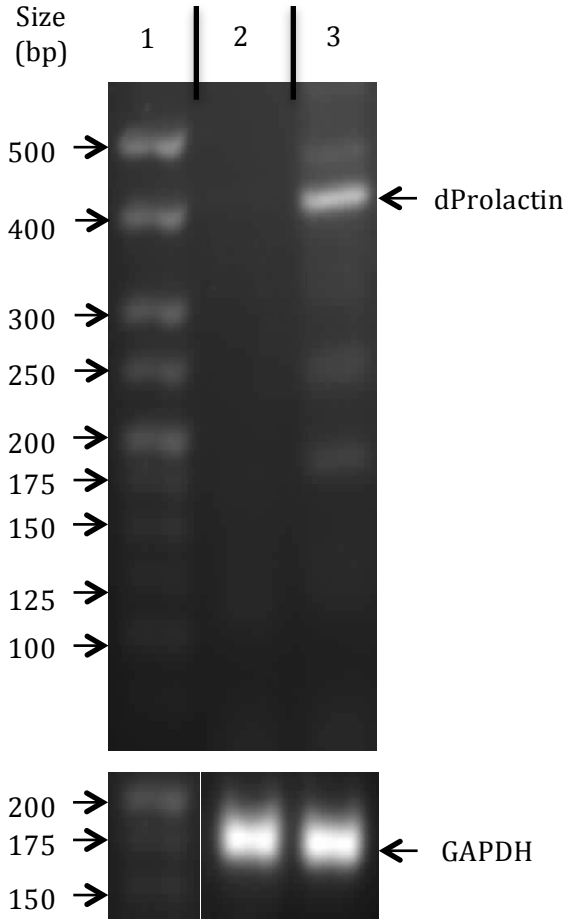

Figure 5: Detection of dProlactin in decidualised St-T1b cells by PCR. Agarose gel showing of dProlactin (416 bp) and GAPDH (159 bp) control with hyper ladder V DNA markers (lane 1) showing dProlactin levels in St-T1b cells stimulated with E2 medium (lane 2) or decidualisation medium (lane 3) for 24 hours. The decidualised St-T1b cells (lane 3) show expression, while no bands are seen in the non-decidualised cells (lane 2).

3.2 VEGF is up-regulated in endometrial stromal cells following decidualisation

Previous studies in this lab have indicated that VEGF is up-regulated in St-T1b cells 3-12 days following decidualisation. To confirm these findings and determine whether increased VEGF expression occurs following shorter exposure of the cells to decidualisation medium the St-T1b cells were grown to confluence and then incubated with either E2 or decidualisation medium. Fresh medium was added to the cells 24 hours prior collection at 24, 48 or 72 hours and VEGF levels assessed by ELISA. High levels of VEGF were detected in the decidualised cells compared to the control cells (Figure 6) within 24 hours of stimulation.

To establish the kinetics of VEGF release from St-T1b, cells were plated on a 12 well plate (1.2×10^5/well) and grown to confluence. They were then treated with decidualisation medium, and conditioned medium collected following 30 minute, 2, 4, 6, 10, and 24 hours incubation and VEGF levels were detected by ELISA. Figure 7 shows the rapid induction of VEGF secretion following stimulation with decidualisation medium, which starts to accumulate rapidly between 6-10 hours.

3.3 Localisation of VEGF and FOXO1 in decidualising St-T1b cells.

To further investigate the induction of VEGF with FOXO1 St-T1b cells were treated with decidualisation medium for between 2 and 24 hours. As a negative control

Figure 6: Up-regulation of VEGF in St-T1b Cells Following Decidualisation

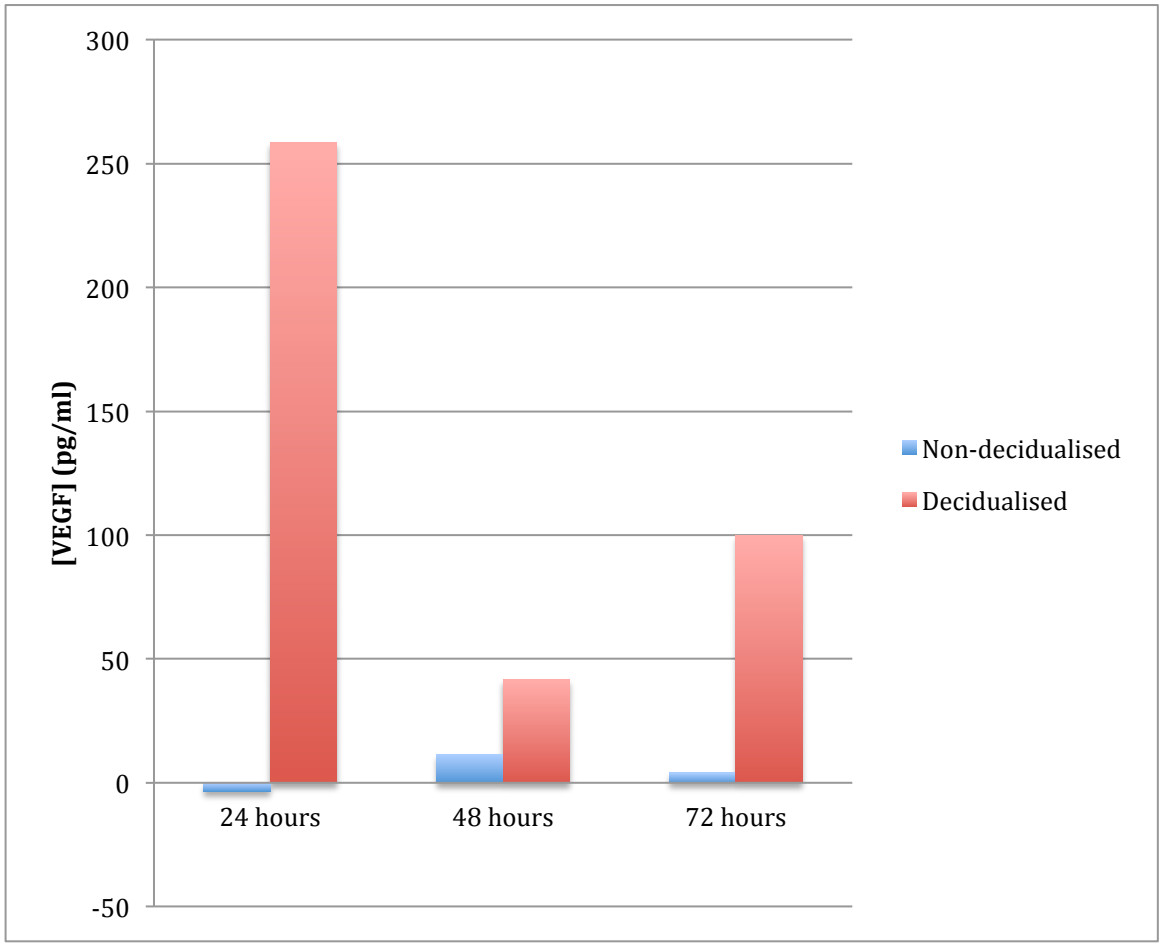

Figure 6: Up-regulation of VEGF in St-T1b cells following decidualisation. St-T1b cells were incubated in decidualising medium (*red bars*) or growth medium (control - *blue bars*) and supernatants were collected over a 24 hour period at various time points. VEGF concentration was determined by ELISA (n=1)

Figure 7: Up-regulation of VEGF in Decidualised St-T1b Cells Over Time

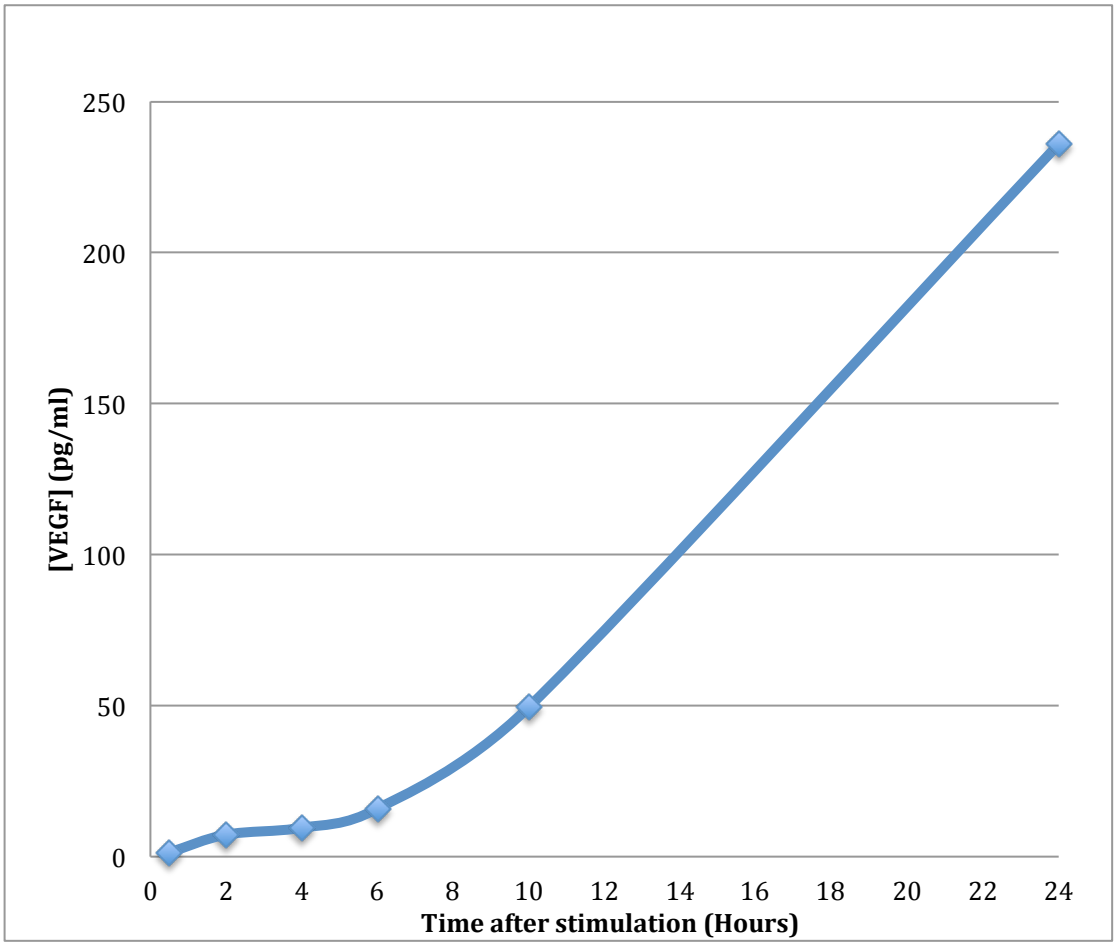

Figure 7: Up-regulation of VEGF in decidualised St-T1b cells over time. VEGF concentration determined by ELISA in decidualised St-T1b cells over a 24 hour time course. (n=1)

St-T1b cells were cultured in E2 medium for 24 hours, and HEC-1B cells used as a as a positive control. St-T1b cells treated with decidualisation medium for 24 hours were used as a negative staining control.

Following stimulation of the cells with decidualisation medium FOXO1 expression increased and it became localised to the nucleus (Figure 8). A clear difference in FOXO1 expression can be seen between the control and decidualised cells with the majority of cells showing strong nuclear staining by 24 hours (Figure 8). This correlates with its role as a transcription factor, initiating downstream effectors of the decidualisation process (Christian et al., 2002). Not all St-T1b cells underwent decidualisation (Figure 8). This is consistent with the complex layering of decidualised and non-decidualised cells seen *in vivo* (Reviewed by Plasier, 2011).VEGF staining was low in the HEC-1B cells which have been found to constitutively secrete VEGF by ELISA (> 100 pg/ml) and some non-specific staining was observed in the negative control making it difficult to interpret the data (Figure 8). However, it was noted that the St-T1b cells that stained strongly for VEGF also showed strong nuclear expression of FOXO1 (Figure 8). The low VEGF expression in the HEC-1B positive control cells suggests that the antibody concentration may have been too low, or that VEGF is exocytosed out of the cell immediately after expression (Figure 8). To investigate this possibility conditioned St-T1b medium was produced and VEGF expression was detected by ELISA.

Figure 8: Localisation of VEGF and FOXO1 in St-T1b Cells

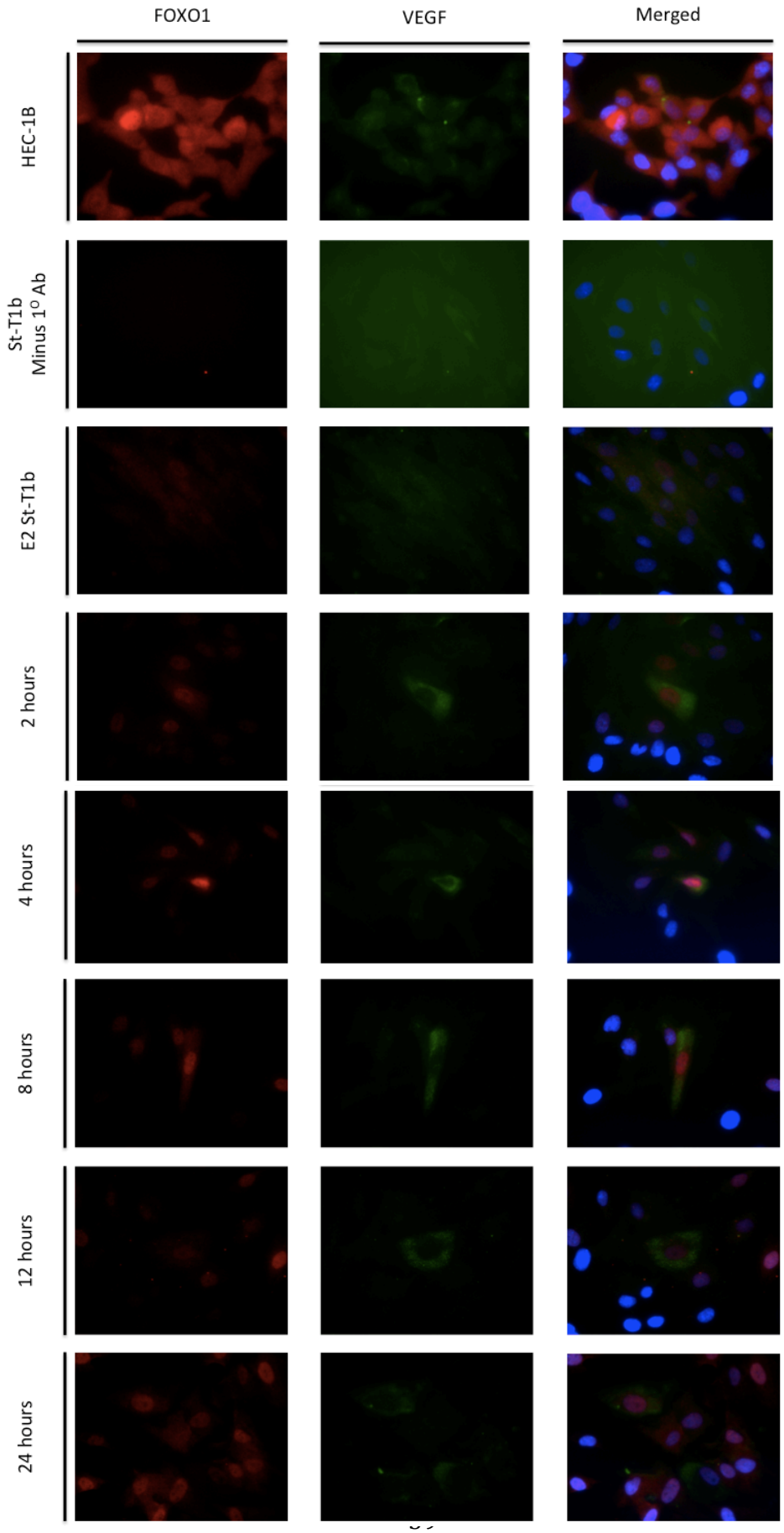

Figure 8: Localisation of VEGF and FOXO1 in St-T1b Cells. FOXO1 fluorescent staining (red), VEGF staining (green) and DAPI staining (blue) x 40 magnification. Positive control was HEC-1B cells, negative control St-T1b cells were incubated without primary antibodies, time in hours correlates to the time stimulated by decidualisation medium.

3.4 FOXO1 increases VEGF promoter activity

To investigate whether FOXO1 can regulate VEGF promoter activity, a plasmid encoding a constitutively active FOXO1 mutant under the control of the CMV promoter (pcDNA3_FOXO1), or empty vector control (pcDNA3) were co-transfected with VEGF promoter luciferase constructs and pRL plasmid (transfection control) into the HEK293 cells. Cells were transfected over a period of 48 hours, and VEGF promoter activity determined by dual luciferase reporter assay. The results were were normalised to Renilla luciferase readings to account for any differences in transfection efficiency in each sample.

.

A greater than two-fold increase of VEGF promoter activity was detected in the presence of FOXO1 for all VEGF promoter reporter plasmids plasmids (Figure 9). This suggests that FOXO1 promotes VEGF expression by interacting with common sites in the first 1.8 Kb upstream of the transcriptional start site.

3.5 Incubation of St-T1b cells with Decidualisation Medium decreases VEGF promoter activity.

The effect of stimulation of St-T1b cells with decidualisation or growth medium on VEGF promoter activity was investigated by a 24 hour transfection of the pGL2-VEGF promoter-luciferase plasmids into St-T1b cells in duplicate, followed by 24 hour

Figure 9: FOXO1 Increases VEGF Promoter Activity

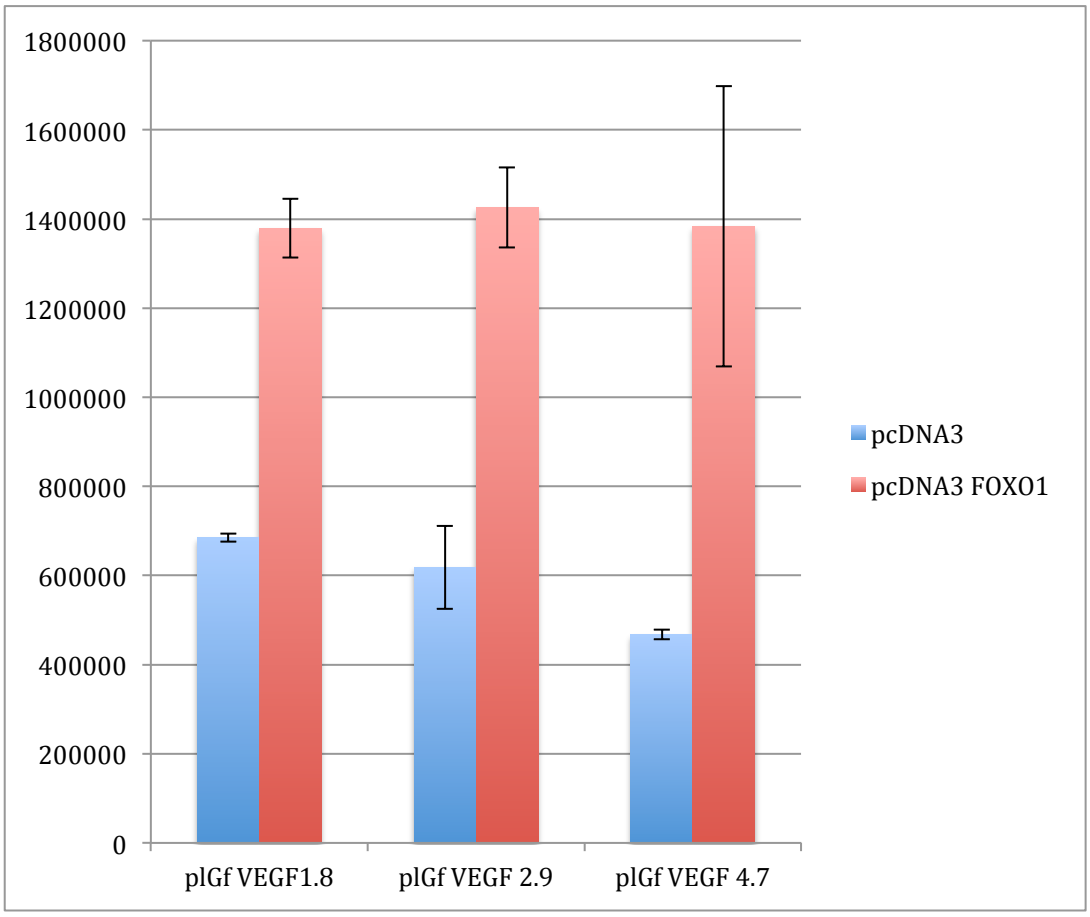

Figure 9: FOXO1 increases VEGF promoter activity. HEK-293 cells co-transfected VEGF reporter-luciferase constructs (pGL2-VEGF-1.8, -2.9, and -4.7) and either pCDNA3-FOXO1 (*red bars*), or empty pCDNA3 plasmd (control – *blue bars*) and incubated for 48 hours. VEGF promoter activity was determined by dual luciferase assay. (n=2)

Figure 10: VEGF Promoter Activity in St-T1b Cells

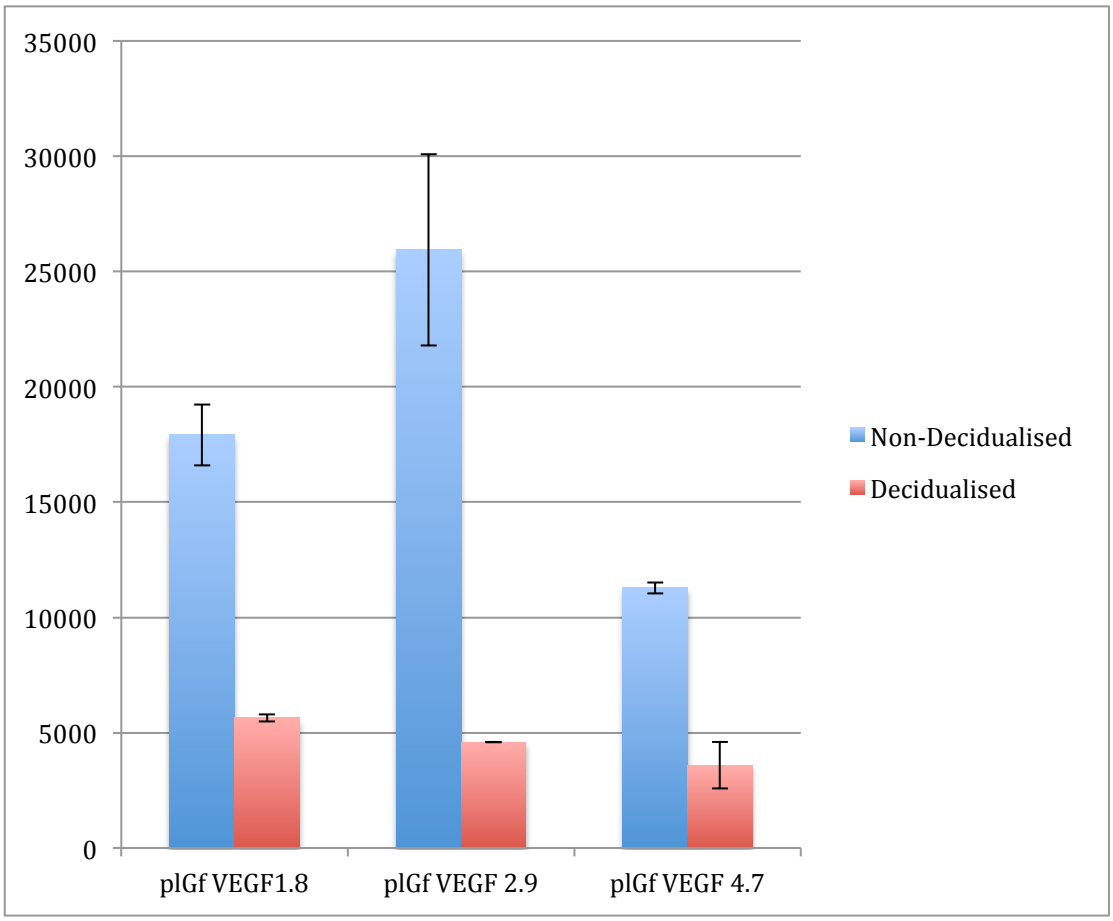

Figure 10: VEGF promoter activity in St-T1b cells. St-T1b cells were cells were transfected VEGF reporter-luciferase constructs (pGL-VEGF-1.8, -2.9, and -4.7) and stimulated with either E2 medium (blue), or decidualisation medium (red) for 24 hours and dual luciferase assay. (n=2)

stimulation with either E2 or decidualisation medium. Again to account for transfection efficiency all transfections were carried out in the presence of the Renilla luciferase plasmid pRL, and data normalised to the Renilla luciferase activity. Surprisingly, a more than 2-fold decrease in VEGF promoter activity was observed in decidualised St-T1b cells compared to non-decidualised cells (Figure 10). This may be due to the much lower transfection rate of St-T1b cells compared to HEK293s, as proliferation rate is much lower in decidualised St-T1b cells, or cAMP in the decidualisation medium may affect other signalling pathways that relate to VEGF expression (Samelocos et al., 2009).

3.6 HTR8 Sprouting Decreases with VEGF Stimulation

To determine the functional implications of VEGF expression by decidual cells, HTR8 cell spheroids were prepared. The HTR8 cells, a trophoblast cell line, were an ideal model for spheroid sprouting studies, and modelled the implanting blastocyst. Between 7-10 spheroids were implanted into fibrinogen, and incubated with low serum growth medium as a control, or low serum growth medium supplemented with either 20 ng/ml VEGF or 100 ng/ml VEGF. Sprouting was monitored over a 72 hour time frame, and bright-field microscopy images at x10 magnification was photographed for analysis (Figure 11). The area of each spheroid (including sprouts) was measured for each image using Image J (Schneider, Rasbind & Eliceiri, 2012),

Figure 11: HTR8 Spheroid Sprouting is reduced with VEGF

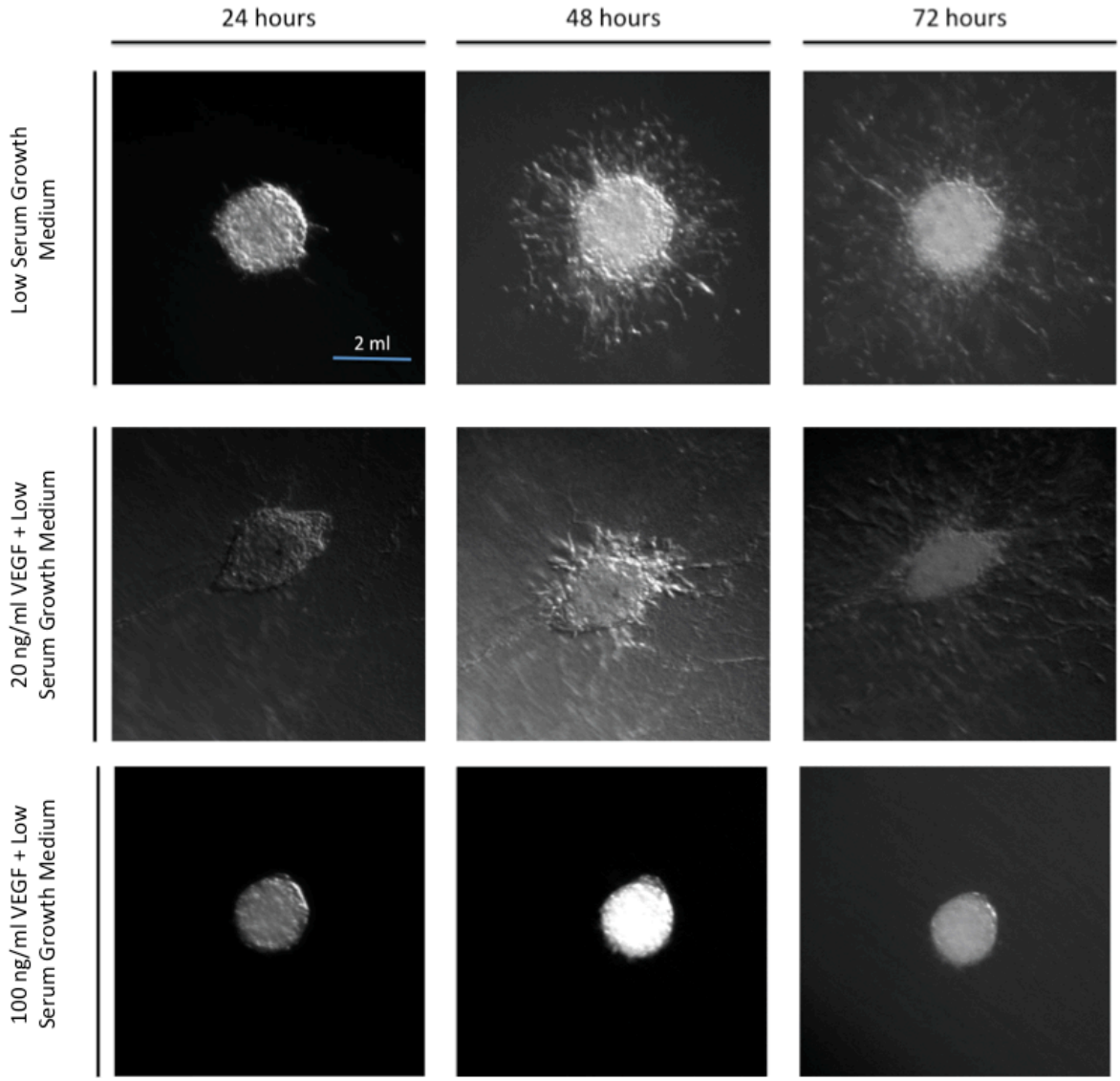

Figure 11: HTR8 spheroid sprouting is reduced with VEGF. Bright-field microscopy images at x10 magnification of HTR8 spheroids taken at 24 hours, 48 hours, and 72 hours of incubation with low serum growth medium control, and low serum growth medium control plus either 20 ng/ml VEGF or 100 ng/ml VEGF. Sprouting become apparent by 48 hours in the control and the 20 ng/ml VEGF medium, sprouting is not observed by 72 hours in the 100 ng/ml VEGF medium.

Figure 12: HTR8 Spheroid Sprouting is inhibited by VEGF

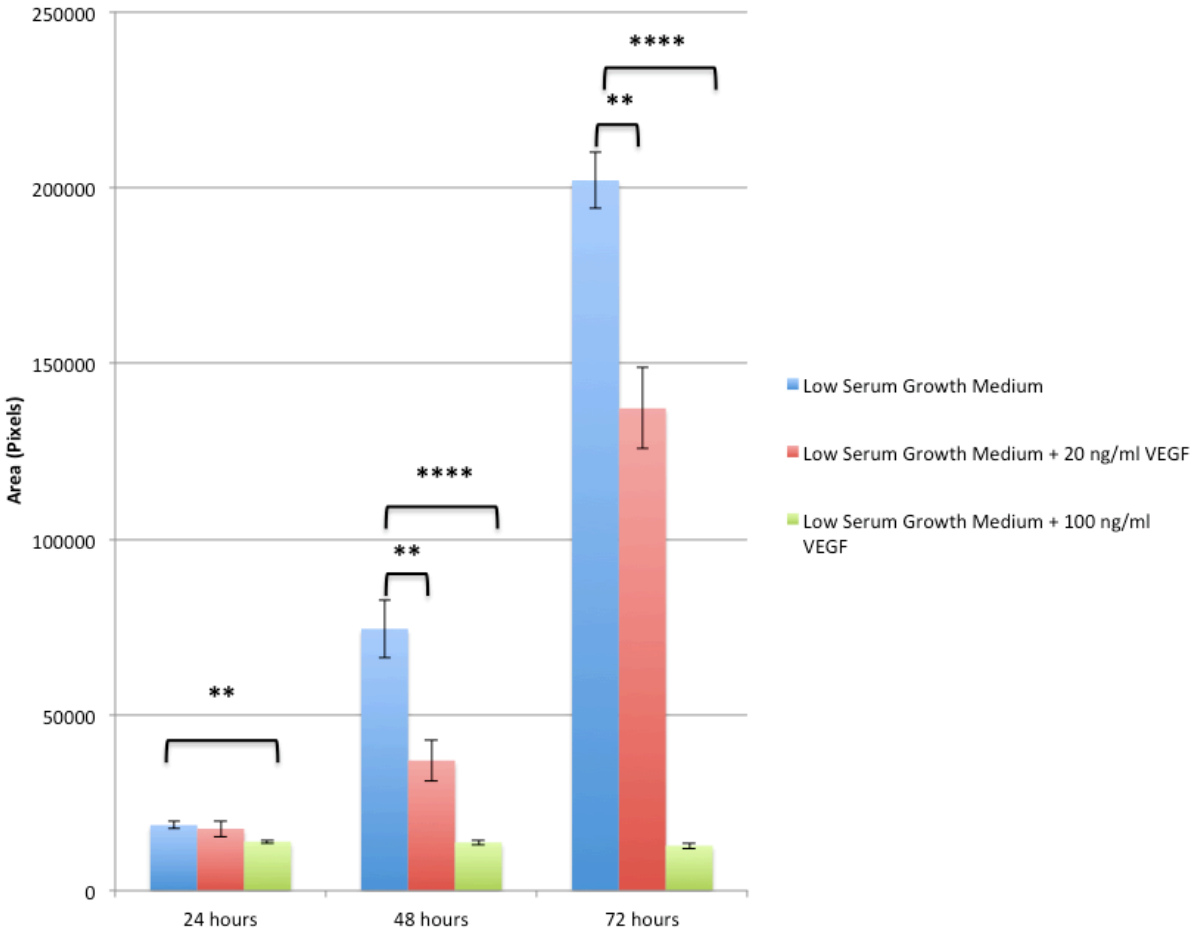

Figure 12: HTR8 spheroid sprouting is inhibited by VEGF. Bar chart showing average area of HTR8 spheroids calculated using Image J, with standard error about the mean. Significant differences were calculated using a two-tailed, paired, students t-test. A p value of 0.00277 was observed between the spheroids incubated with low serum control and low serum control plus 20 ng/ml VEGF at 48 hours, and of 0.00123 at 72 hours. A p value of 0.00277 was observed between the low serum control and the low serum growth medium plus 100 ng/ml VEGF at 24 hours, of 6.02×10^{-5} at 48 hours and of 2.6×10^{-6} at 72 hours.

Figure 10 indicates that sprouting in both the low serum, and 20 ng/ml VEGF spheroids became apparent by 48, whereas the spheroids incubated with 100 ng/ml VEGF failed to produce sprouts by 72 hours. Each condition had an n number of between 7-11, the average area of the spheroids for each condition was calculated and plotted in Figure 12. Figure 12 shows a significant difference, where $p<0.01$, between the low serum control, and the 20 ng/ml VEGF spheroids at both the 48 hour and 72 hour time point. A significant difference between the areas of spheroids incubated with the low serum growth medium and the 100 ng/ml VEGF medium can also be observed (Figure 12). With a p value of less than 0.01 at 24 hours, and a p value of less than 0.0001 at the 48 hour and 72 hour time points, suggesting that high levels of VEGF may inhibit trophoblast invasion (Figure 12). To investigate this further spheroids were incubated with E2 growth medium, and conditioned day 9 decidual cell medium.

3.7 HTR8 Sprouting Decreases when Incubated with E2 and Conditioned Decidualisation Medium

Following on from the HTR8 spheroid incubation with VEGF, spheroids were incubated with a low serum growth medium control, the E2 growth medium, and conditioned medium from day 9 decidual cells (Figure 13 and 14). Figure 12 shows that in all conditions sprouting to a certain degree can be seen by 48 hours.

Analysis of the data indicates that there is a significant difference of $p<0.01$ between the low serum control and E2 medium at 48 and 72 hours (Figure 14). A

Figure 13: HTR8 Spheroid Sprouting is reduced with Decidualised St-T1b Medium

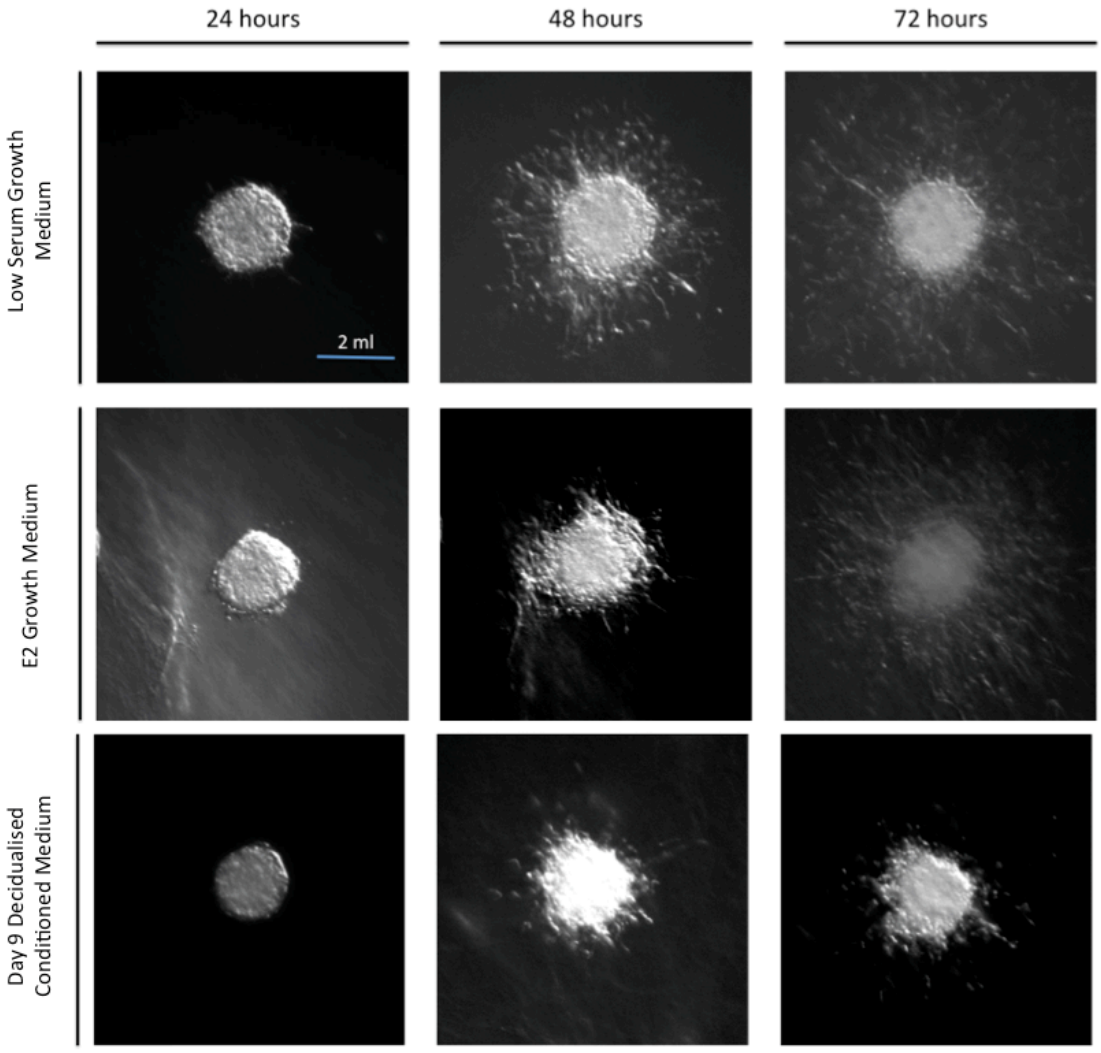

Figure 13: HTR8 spheroid sprouting is reduced with decidualised St-T1b medium. Bright-field microscopy images at x10 magnification of HTR8 spheroids taken at 24 hours, 48 hours, and 72 hours of incubation with low serum growth medium control, E2 growth medium and conditioned medium from day 9 decidual cells. Sprouting becomes apparent by 48 hours in the all conditions.

Figure 14: Decidualised St-T1b medium inhibits HTR8 Sphroid Sprouting

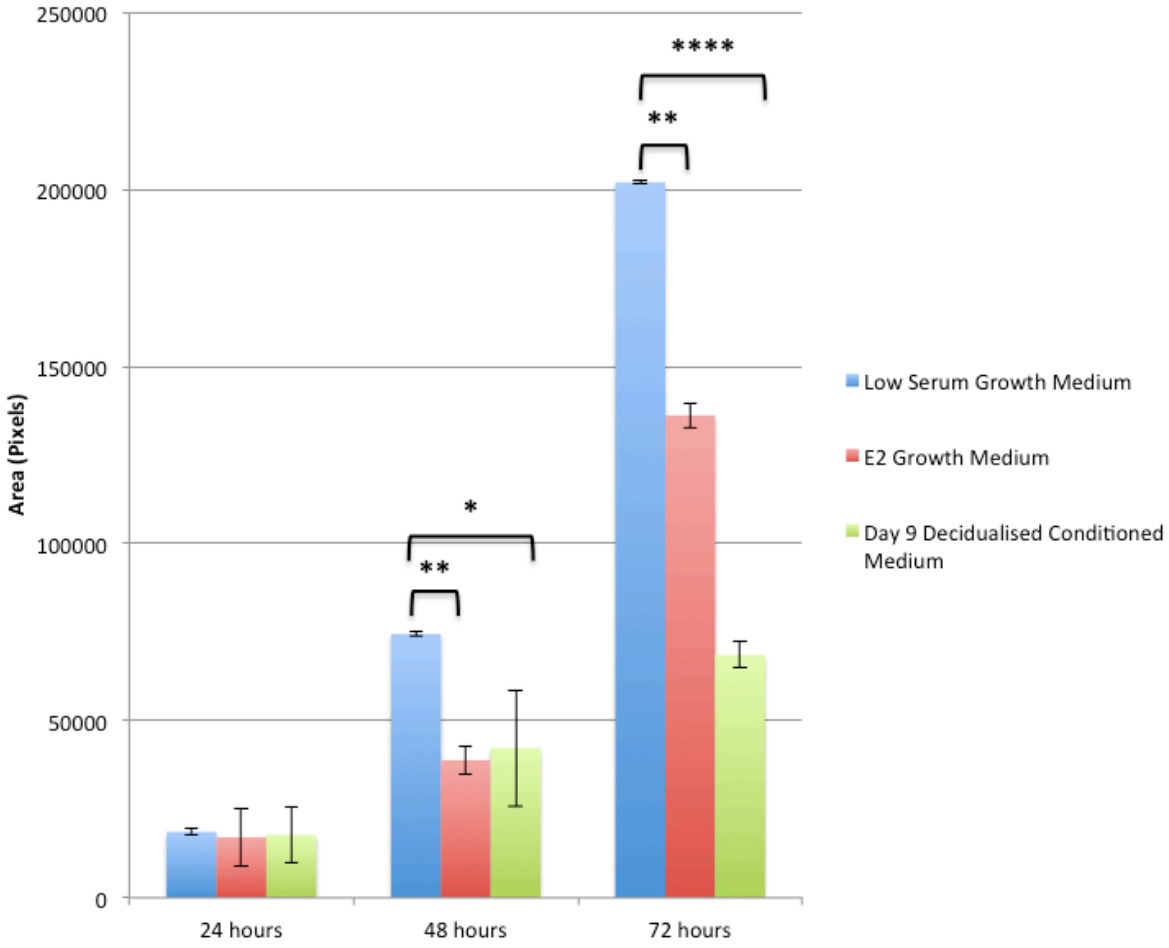

Figure 14: HTR8 spheroid sprouting is inhibited by decidualised St-T1b medium. Bar chart showing average area of HTR8 spheroids calculated using Image J, with standard error about the mean. Significant differences were calculated using a two-tailed, paired, students t-test. A p value of 0.00269 was observed between the spheroids incubated with low serum control and E2 growth medium VEGF at 48 hours, and of 0.00552 at 72 hours. A p value of 0.00507 was observed between the low serum control and the conditioned medium from day 9 decidual cells at 48 hours and of 3.98×10^{-9} at 72 hours.

significant difference between the low serum control and conditioned medium can also be observed, with a p value of less than 0.05 at 48 hours and less than 0.0001 at 72 hours (Figure 14). This also supports the notion that VEGF may act to regulate trophoblast invasion.

4.0 Discussion

VEGF is integral for vascular remodelling during decidualisation, and for sustaining blood supply to the growing embryo (Plasier et al., 2011). Expression has been reported in primary endometrial stomal cells, primary endometrial decidual cells, and the stromal cell line St-T1b when under decidualisation conditions (Sugino et al., 2002; Popovici et al., 1999; Schwenke et al., 2013). Along with being an angiogenic factors, it has also been reported to play a role in induction of cell survival pathways (Spyridopoulous et al., 1996; Gerber et al., 1998; Gerber et al., 1998). Much is known about VEGF's function in vascular remodelling, however very little is known about its significance, and thus implications of its expression in decidual cells. This project hypothesised that VEGF is expressed upon decidualisation of stromal cells in response to cAMP pathways; results support this hypothesis and suggest potential functional consequences of VEGF expression.

The St-T1b endometrial stromal cell-line was used as a model for decidual cells, as they decidualise upon stimulation with progesterone and cAMP containing medium (Samaleacos et al., 2009). The low n number for some of the experiments can be explained by the difficulty in inducing decidualisation at first. The cells were proliferating very slowly, and not reaching confluence when expected, therefore slowing down the rate at which experiments could be carried out at. This problem was remedied with the addition of insulin, and new foetal bovine serum (Sigma) after which the condition of the cells improved vastly and readily underwent decidualisation.

As mentioned previously, past studies have observed changes in VEGF expression levels between primary endothelial stromal and decidual cells (Sugino et al., 2002; Popovici et al., 1999). Although high levels of VEGF have also been recorded in decidualised St-T1b cells a direct comparison of VEGF expression in non-decidualised and decidualised St-T1b cells has not been explored (Schwenke et al., 2013). Detection of VEGF by ELISA in conditioned medium found that VEGF levels rapidly increase after 24 hours of stimulation with decidualisation medium. Increases were also observed at 48 and 72 hours, but to a lesser extent. This decrease may have been because the cells became exhausted after consecutive stimulation with cAMP and progesterone over 24 hours. Ideally the ELISA would be repeated at least two more times to get an n number of 3, however due to the difficulties at the beginning of the project this was only carried out once. However, the short time course experiment measured by ELISA, and previously unpublished ELISA data carried out within the lab also support these findings. These results correlate to the large induction of VEGF expression found in immune cells that localise to the endometrium during decidualisation (Charnock-Jones et al., 2000; Mueller et al., 2000; Li et al., 2001; Jabbour et al., 2006).

In order to investigate a potential relationship between FOXO1 and VEGF expression fluorescence staining was carried out. The increase in FOXO1 staining in decidual St-T1b cells compared to non-decidualised cells is supported in the literature, and the nuclearisation of FOXO1 in response to cAMP stimulation could also be observed (Christian et al., 2002; Labied et al., 2006). The VEGF staining proved more difficult to interpret. Whereas the FOXO1 positive and negative controls were to a good standard, the positive and negative controls for VEGF were poor. Little staining could

be observed in the positive control, and non-specific staining could be seen in the negative control. Despite this, in the merged images VEGF staining tended to be localised to cells that also had nuclear FOXO1 staining, and also appeared to be vesicular in nature. The low VEGF staining in the positive control could be explained if VEGF is rapidly secreted, the staining protocol could be improved in the future by addition of sodium azide to the fixative solution in order to retain any secretory proteins within the cells during the washes.

Luciferase reporter assays in HEK293 cells showed a large increase in exogenous VEGF expression when co-transfected with FOXO1. This supports unpublished data from the lab in which cells infected with a constitutively active FOXO1 adenovirus rapidly produced high levels of VEGF. Suggesting a role for FOXO1 in VEGF expression. However, this was not supported by the luciferase reporter assay carried out in non-decidualised and decidualised St-T1b cells. Exogenous VEGF levels decreased in decidualised cells, which is contradictory to the previous findings. This may have been due to other factors stimulated by cAMP, or because St-T1b cell proliferation was stimulated by FGF during transfection and may have interfered with cellular pathways. Ideally the transfection process would be optimised, and negative control wells without stimulation with FGF used to rule out any interference. Another possibility could be that like prolactin, VEGF may have an alternative promoter site specific to decidualisation (Pohnke, Kempf & Gellerson, 1999; Christian et al., 2002). The VEGF gene is 16.3 kb, the plasmids used in the luciferase reporter assays only had a maximum VEGF insert of 4.7 kb, therefore there may be other promoter regions in the remaining 11.6 kb.

Together, the HEK293 luciferase assay results and the fluorescence staining are indicative of a relationship between nuclear localisation of FOXO1 and VEGF expression. Furayama et al. (2004) described FOXO1 as vital for VEGF mediated vascularisation during development. Distinct morphological differences were observed in endothelial cells of FOXO1 deficient mice. The mice were not viable, and had irregular vascular development caused by abnormal VEGF expression in response to the FOXO1 knock out (Furayama et al., 2004). More recently, FOXO1 was found to bind the VEGF-A promoter and regulate gene expression directly in Pancreas β-Cells, which supports the hypothesis made by this study that VEGF expression in decidual cells may be regulated by cAMP induced mechanisms, such as FOXO1 (Kikuchi et al., 2012).

To determine functional implications of VEGF expression, HTR8 spheroids were used as a model for the outer layer of trophoblasts of the blastocyst. During implantation trophoblasts adhere to the endometrium, and implant in an invasive manner (Plasier et al., 2011). Trophoblast cells are known to secrete VEGF to promote angiogenesis at the site of implantation, however the effects of externally produced VEGF upon stromal cells have not been studied in any great detail (Plasier et al., 2011). Spheroids were incubated with a control low serum medium and either increasing concentrations of VEGF, or with either non-decidualising E2 medium, or day 9 decidualisation conditioned medium. Both concentrations of VEGF inhibited sprouting of HTR8 cells at the 48 and 72 hour time points to a level of statistical significance. This was particularly evident in the spheroids incubated with 100 ng/ml VEGF, which gave a p value of 2.6×10^{-6} by the 72 hour time point. Similar decreases were observed

in the spheroids incubated with either E2 growth medium, or day 9 decidualisation conditioned medium. A p value of 3.98×10^{-9} was observed at 72 hours for the spheroids incubated with the day 9 decidualisation conditioned medium. This data suggests a functional role for VEGF other than that observed in angiogenesis and perhaps is involved in regulation of invasion processes. This is supported by the expression of VEGF receptor Flt1 and KDR by trophoblast cells (Shore et al., 1997).

In respect to future research avenues, ideally RT-PCR to analyse mRNA levels of VEGF during decidualisation would be carried out, to establish whether the high concentration of VEGF detected by ELISA was due to expression or excretion of VEGF stores within the cell. Chromatin Immunoprecipitation (or ChIP) analysis of VEGF and FOXO1 would elucidate whether FOXO1 regulates VEGF expression in a direct manner. Ultimately, stable knock down of FOXO1 in St-T1b cells with siRNA would create an ideal negative control and would provide a more accurate way of assessing the effect of FOXO1 on VEGF expression. In respect to functional analysis, invasion assays using matrigel inserts may provide a way to assess spheroid invasion in response to VEGF or conditioned medium. The findings of this project support the hypothesis that VEGF expression increases with decidualisation of St-T1b cells, and is potentially regulated by FOXO1. In respect to the literature, the high VEGF expression by the decidualised St-Tb cells along with the known expression of Flt1 and KDR by primary decidual cells could implicate VEGF as an autocrine survival signal (Shore et al., 1997). The response of the HTR8 spheroids to incubation with VEGF, and conditioned decidual medium suggest possible functional mechanisms. This project has only

scratched the surface of the role of VEGF in decidualisation and further research is required to elucidate its role, and the mechanisms by which it functions.

5.0 References

Brar AK, Handwerger S, Kessler CA and Aronow BJ (2001) Gene induction and categorical reprogramming during in vitro human endometrial broblast decidualization. *Physiological Genomics* **7** 135–148.

Brosens JJ and Gellerson B (2006) Death or survival-a progesterone dependent cell fate decisions in the human endometrial stroma. *Journal of Molecular Endocrinology*, **36** 389-398

Charnock-Jones DS, Macpherson AM, Archer DF, Leslie S, Makkink WK, Sharkey AM and Smith SK (2000) The effect of progestins on vascular endothelial growth factor, oestrogen receptor and progesterone receptor immunoreactivity and endothelial cell density in human endometrium. *Human Reproduction*, **15** (Suppl. 3) 85-95

Christian M, Zhang X, Schneider-Merck T, Unterman TG, Gellerson B, White JO and Brosens JJ (2002) Cyclic AMP-induced forhead transcription factor, FKHR, cooperates with CCAAT/enhancer-binding protein beta in differentiating human endometrial stromal cells. *Journal of Biological Chemistry,* **277** (23) 20825-20832

Daly DC, Maslar IA and Riddick DH (1983) Prolactin production during in vitro decidualization of proliferative endometrium. *American Journal of Obstetrics and Gynecology* **145** 672–678

Davies RJ, Bennicelli JL, Macina RA, Nycum LM, Biegel JA and Barr FG (1995) Structural characterisation of the FKHR gene and its rearrangement in alveolar rhabdomyosarcoma. *Human Molecular Genetics,* **4** (12) 2355-2362

Furuyama T, Kitayama K, Shimoda Y, Ogawa M, Sone K, Yoshida-Araki K, Hisatsune H, Nishikawa S, Nakayama K, Nakayama K, Ikeda K, Motoyama N and Mori N (2004) Abnormal angiogenesis in FOXO1 (Fkhr) deficient mice. *Jounral of Biological Chemistry,* **279** (33) 34741-34749

Gellerson B and Brosens J (2003) Cyclic AMP and progesterone receptor cross-talk in human endometrium: a decidualising affair. *Journal of Endocrinology*, **178** 357-372

Gerber, H., Dixit, V. & Ferrara, N. (1998) Vascular endothelial growth factor induces expression of the antiapoptotic proteins Bcl-2 and A1 in vascular endothelial cells. *The Journal of biological chemistry*. **273** (21) p.13313–13316

Gerber, H., McMurtrey, A., Kowalski, J. and Yan, M., *et al.* (1998) Vascular endothelial growth factor regulates endothelial cell survival through the phosphatidylinositol 3'-kinase/Akt signal transduction pathway. Requirement for Flk-1/KDR activation. *The Journal of biological chemistry*. **273** (46) p.30336–30343.

Graham CH, Hawley TS, Hawley RC, MacDougall JR, Kerbel RS, Khoo N and Lala PK (1993) Establishment and characterisation of first trimester human trophoblast cells with extended lifespan. *Experimental Cell Research*, **206** (2) 204-211

Graham FL and Smiley J (1977) Characteristics of a human cell line transformed by DNA from human adenovirus type 5. *J Gen Virol*, **36** 59-74

Hinrichsen MJ and Blaquier JA (1980) Evidence supporting the existence of sperm maturation in the human epididymis. *J Reprod Fertil,* **60** 291-294

Jabbour HM, Kelly RW, Fraser HM and Critchley HOD (2006) Endocrine regulation of menstruation. *Endocrine Reviews*, **27** (1) 17-46

Johnson MH and Everitt BJ (2007) *Essential Reproduction*. Sixth Edition. Oxford: Blackwell Publishing

Kaji K and Kuda A (2004) The mechanism of sperm-oocyte fusion in mammals. *Reproduction*, **127** 423-429

Katoh M (2004) Human FOX gene family (Review). *International Journal of Oncology*, **25** (5) 1495-1500

Kikuchi O, Kobayashi M, Amano K, Sasaki T, Kitazumi T, Kim HY, Lee YS, Yokota-Hasimoto H, Kitamura YI and Kitamura T (2012) FoxO1 gain of function in the pancreas causes glucose intolerance, polycystic pancreas, and islet hypervascularisation. *PLos ONE,* **7** (2) e32249

Korff T and Augustin HG (1998) Integration of endothelial cells in multicellular spheroids prevents apoptosis and induces differentiation. *Journal of Cell Biology*, **143** (5) 1341-1352

Kuramoto H and Hamano M (1977) Etablishmen and characterisation of the cell line of a human endometrial adenocanthoma. *Eur J Cancer,* **13** 253-259

Labied S, Kajihara T, Madureira PA, Fusi L, Jones MC, Higham JM, Varshochi R, Francis JM, Zoumpoulidou G, Essafi A, de Mattos SF, Lam EWF and Brosens JJ (2006) Progestins regulate the expression and activity of the forkhead transcription factor FOXO1 in differentiating human endometrium. *Molecular Endocrinology*, **20** (1) 35-44

Landschulz WH, Johnson PF and McKnight SL (1998) The leucine zipper: a hypothetical structure common to a new class of DNA binding proteins. *Science,* **240** 1759-1794

Li XF, Charnock-Jones DS, Zhang E, Hiby S, Malik S, Day K, Licence D, Bowen JM, King A, Loke YW and Smith SK (2001) Angiogenic growth factor messenger ribonucleic acids in uterine natural killer cells. *J Clin Endocrinol Metab,* **86** 1823-1834

Malizia BA, Hacker MR and Penzias AS (2009) Cumulative live-birth rates after in vitro fertilisation. *New England Medical Journal*, **360** 236-243

Mihm M, Gangooly S and Muttukrishna S (2010) The normal menstrual cycle in women. *Anim Reprod Sci*, **134** (3-4) 229-236

Mueller MD, Lebovic DI, Garret R and Taylor RN (2000) Neutrophils infiltrating the endometrium express vascular endothelial growth factor: potential role in endometrial angiogenesis. *Fertil Steril,* **74** 107-112

Noorwood JT, Hein CE, Halbert SA and Anderson RG (1978) Polycationic molecules inhibit cilia-mediated ovum transport in the rabbit oviduct. *PNAS*, **75** (9) 4413-4416

Oliver C, Montes MJ, Galindo JA, Ruiz C and Olivares EG (1999) Human decidual stromal cells express alpha-smooth muscle actin and show ultrastructural similarities with myobroblasts. H*uman Reproduction* **14** 1599–1605.

Olsson P and Laska M (2010) Human male superiority in olfactory sensitivity to sperm attractant odorant bourgeonal. *Chem Senses,* **35** (5) 427-432

Osman RA, Andria ML, Jones D and Meizel S (1989) Steroid induced exocytosis: the human sperm acrosome reaction. *BBRC*, **160** (2) 828-833

Plaisier M (2011) Decidualisation and angiogenesis. *Clinical obstetrics and gynaecology*, **25** (3) 259-271

Pohnke Y, Kempf R and Gellerson B (1999) CCAAT/enhancer binding proteins are mediators in the protein kinase A dependent activation of the decidual prolactin promoter. *Journal of Biological Chemistry*, **274** (35) 24808-24818

Popovici RM, Irwin JC, Giaccia AJ and Giudice LC (1999) Hypoxia and cAMP stimulate cascular endothelial growth factor (VEGF) in human endometrial stromal cells: potential relevance to menstruation and endometrial regeneration. *Journal of Clinical Endocrinology and Metabolism*, **84** (6) 2245

Psychoyos, A. (1976) Hormonal control of uterine receptivity for nidation. J. *Reprod. Fertil.,* **25**, (Suppl.) 17-28.

Puissant F, Van Rysselberge M, Barlow P, Dewese J, and Leroy F (1987) Embryo scoring as a prognostic tool in IVF treatment. *Human Reproduction*, **2** (8) 705-708

Salicioni AM, Platt MD, Wertheimer EV, Arcelay E, Allaire A, Sosnik J and Visconti PE (2007) Signalling pathways involved in sperm capacitation, *Spermatology*, **65** 245-260

Samalecos A, Reinmann K, Wittmann S, Sculte HM, Brosens JJ, Bamberger AM and Gellerson B (2009) Charachterisation of a nocel telomerase-immortalised human endomertrial cell line St-T1b. *Reprod Bio Endocrinol*, **7** 76

Schneider CA, Rasband WS and Eliceiri KW (2012) NIH image to ImageJ: 25 years of images analysis. *Nature Methods,* **9** 671-675

Schwenke M, Knöfler M, Velicky P, Weimar CHE, Kruse M, Samalecos A, Wolf A, Macklon NS, Bamberger AM and Gellerson B (2013) Control of human endometrial cell motility by PGDF-BB, HB-EGF and trophoblast-secreted factors. *PLoS-ONE,* **8** (1) e54336

Shore VH, Wang TH, Wang CL, Torry RJ, Caudle MR and Torry DS (1997) Vascular endothelial growth factor, placenta growth factor and thei receptors in isolated human trophoblasts. *Placenta***, 18** (8) 657-665

Spyridopoulos I, Brogi E, Kearney M, Sullican AB, Cetrulo C, Isner JM and Losordo DW (1996) Vascular endothelial growth factor inhibits endothelial cell apoptosis induced by tumour necrosis factor alpha: balance between growth and death signals. *Journal of Molcular and Cellular Cardiology*, **29** (5) 1321-1330

Steptoe P and Edwards R (1978) Birth after the reimplantation of a human embryo. *Lancet*, **2** (8085) 366

Straussman BI (1998) Energy enconomy in the evolution of menstruation. *Eolutionary Anthropology*, **5** (5) 157-164

Sugino N, Kashida S, Karube-Harada A, Takiguchi S and Kato H (2002) Expression of vascular endothelial growth factor (VEGF) and its receptors in human endometrium throughout the menstrual cycle and in early pregnancy. *Reproduction,* **123** 379-387

Tanaka N, Miyazaki K, Tashiro H, Mizutani H and Okamura H (1993) Changes in adenylyl cyclase activity in human endometrium during the menstrual cycle and in human decidua during pregnancy. *Journal of Reproduction and Fertility*, **97** 33-39

Tang ED, Nuñez G, Barr FG and Guan KL (1999) Negative regulation of the forkhead transcription factor FKHR by Akt. *Journal of Biochemical Chemisry,* **274** (24) 16741-16746

Telgmann R and Gellerson B (1998) Marker genes of decidualisation: activation of the decidual prolactin gene. *Human Reproduction Update*, **4** (5) 472-479

Telgmann R, Maronde E, Takén K and Gellerson B (1997) Activated protein kinase A is required for differentiation dependent transcription of the decidual prolactin gene in human endometrial stromal cells. *Endocrinology*, **138** (3) 929-937

Tseng L, Gao JG, Chen R, Zhu HH, Mazella J and Powell DR (1992) Effect of progestin, antiprogestin, and relaxin on the accumulation of prolactin and insulin-like growth factor-binding protein-1 messenger ribonucleic acid in human endometrial stromal cells. *Biology of Reproduction* **47** 441–450.